AD-A190 688 SYNTHETIC-APERTURE RADARS VIEWED AS INTERFEROMETERS WITH MATCHED FILTER P... (U) AIR FORCE WRIGHT AERONAUTICAL LABS WRIGHT-PATTERSON AFB OH... 1/1

UNCLASSIFIED E B CHAMPAGNE MAY 87 AFWAL-TR-86-1160 F/G 17/9 NL

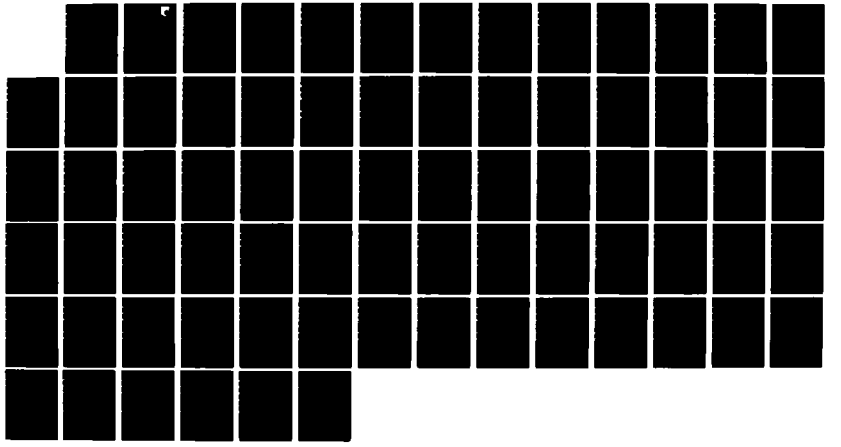

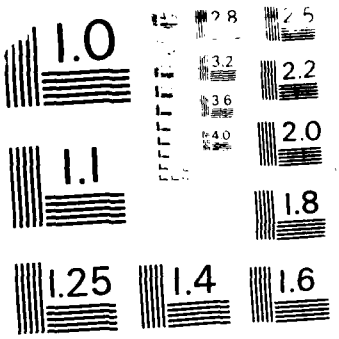

AFWAL-TR-86-1160

SYNTHETIC-APERTURE RADARS VIEWED AS INTERFEROMETERS WITH MATCHED FILTER PROCESSING OF THE COLLECTED DATA

Dr. Edwin B. Champagne
Electronic Technology Division

May 1987

Final Report for Period October 1986 - November 1986

Approved for public release; distribution unlimited.

AVIONICS LABORATORY
AIR FORCE WRIGHT AERONAUTICAL LABORATORIES
AIR FORCE SYSTEMS COMMAND
WRIGHT-PATTERSON AIR FORCE BASE, OHIO 45433-6543

NOTICE

When Government drawings, specifications, or other data are used for any purpose other than in connection with a definitely Government-related procurement, the United States Government incurs no responsibility or any obligation whatsoever. The fact that the Government may have formulated or in any way supplied the said drawings, specifications, or other data, is not to be regarded by implication, or otherwise in any manner construed, as licensing the holder, or any other person or corporation; or as conveying any rights or permission to manufacture, use, or sell any patented invention that may in any way be related thereto.

This report has been reviewed by the Office of Public Affairs (ASD/PA) and is releasable to the National Technical Information Service (NTIS). At NTIS, it will be available to the general public, including foreign nations.

This technical report has been reviewed and is approved for publication.

Edwin B. Champagne

EDWIN B. CHAMPAGNE, Actg Chief
Electronic Research Branch
Electronic Technology Division

FOR THE COMMANDER

WILLIAM J. EDWARDS, Director
Electronic Technology Division
Avionics Laboratory

If your address has changed, if you wish to be removed from our mailing list, or if the addressee is no longer employed by your organization please notify AFWAL/AADR , Wright-Patterson AFB, OH 45433-6543 to help us maintain a current mailing list.

Copies of this report should not be returned unless return is required by security considerations, contractual obligations, or notice on a specific document.

REPORT DOCUMENTATION PAGE

1a. REPORT SECURITY CLASSIFICATION: Unclassified	1b. RESTRICTIVE MARKINGS
2a. SECURITY CLASSIFICATION AUTHORITY	3. DISTRIBUTION/AVAILABILITY OF REPORT: Approved for public release; distribution unlimited
2b. DECLASSIFICATION/DOWNGRADING SCHEDULE	
4. PERFORMING ORGANIZATION REPORT NUMBER(S): AFWAL-TR-86-1160	5. MONITORING ORGANIZATION REPORT NUMBER(S)
6a. NAME OF PERFORMING ORGANIZATION: Electronic Technology Division; 6b. OFFICE SYMBOL (If applicable): AFWAL/AAD	7a. NAME OF MONITORING ORGANIZATION
6c. ADDRESS (City, State and ZIP Code): AFWAL/AAD, Wright-Patterson AFB OH 45433-6543	7b. ADDRESS (City, State and ZIP Code)
8a. NAME OF FUNDING SPONSORING ORGANIZATION: Electronic Technology Division; 8b. OFFICE SYMBOL (If applicable): AFWAL/AAD	9. PROCUREMENT INSTRUMENT IDENTIFICATION NUMBER
8c. ADDRESS (City, State and ZIP Code): AFWAL/AAD, Wright-Patterson AFB OH 45433-6543	10. SOURCE OF FUNDING NOS.

PROGRAM ELEMENT NO	PROJECT NO	TASK NO	WORK UNIT NO
62204F	2001	05	05

11. TITLE (Include Security Classification): Synthetic-Aperture Radars Viewed As Interometers With (continued)

12. PERSONAL AUTHOR(S): Dr Edwin B. Champagne

13a. TYPE OF REPORT	13b. TIME COVERED	14. DATE OF REPORT (Yr., Mo., Day)	15. PAGE COUNT
Final	FROM Oct 86 TO Nov 86	1986 October 29	73

16. SUPPLEMENTARY NOTATION

17. COSATI CODES			18. SUBJECT TERMS (Continue on reverse if necessary and identify by block number)
FIELD	GROUP	SUB GR	
23	05		Synthetic-Aperture Radar, Matched Filtering, Polar Formatting; Fast Fourier Transforms, Backprojection Processing
17	09		

19. ABSTRACT (Continue on reverse if necessary and identify by block number)

In this report we attempted to characterize a Synthetic-Aperture Radar in its most basic physical form and to illustrate the characteristics of various engineering approaches to the implementation of a working system. The rationale for this approach being a separation of the physical attributes from the engineering attributes as the distinction has become, or always was, rather muddled and as such may stifle thought on implementation approaches and perhaps even applications of SAR. Much of the present activity in the SAR area centers on data forms, and we have illustrated that these are processing or implementation concerns and not basic radar concerns. Thus, there may be preferred ways to implement processing schemes to achieve some end, but there are probably alternatives which will achieve the same end. Perhaps this separation of the fundamentals and the engineering aspects will afford the opportunity for more approaches to be proposed. At least it may provide a better understanding of SAR. I feel the approach has helped me in this regard.

This report contains sections dealing with various aspects of a SAR and provides various levels of detail. [Continued on Reverse]

20. DISTRIBUTION/AVAILABILITY OF ABSTRACT	21. ABSTRACT SECURITY CLASSIFICATION
UNCLASSIFIED/UNLIMITED ☒ SAME AS RPT ☐ DTIC USERS ☐	Unclassified

22a. NAME OF RESPONSIBLE INDIVIDUAL	22b. TELEPHONE NUMBER (Include Area Code)	22c. OFFICE SYMBOL
Dr Edwin B. Champagne	513-255-3075	AFWAL/AAD

DD FORM 1473, 83 APR — EDITION OF 1 JAN 73 IS OBSOLETE

11. Title (continued)
Matched Filter Processing Of The Collected Data.

19. Abstract (continued)
For the most part they can be treated as addressing three aspects of SAR and read individually. Introductory sections are devoted to the interferometer and matched filter concepts basic to SAR. Secondary sections provide a description of traditional range-azimuth formatting approaches to matched filtering, and go on to describe the polar formatting process conceived to alleviate the shortcoming of the range-azimuth format. The final sections deal with various digital and optical implementations which are being, or can be used, to perform the final reduction of polar formatted residue data. This process is basically a 2-D Fourier-Transform process. Topics covered include the FFT, interpolation, and back projection processing.

ACKNOWLEDGMENTS

The author wishes to acknowledge the helpful encouragement of his colleagues over the years and, in particular, the continual encouragement of William J. Edwards. A special thanks goes to Nicki Selegan for her translation and transcription of many illegible handwritten drafts, and her patient rework of the many iterations.

CONTENTS

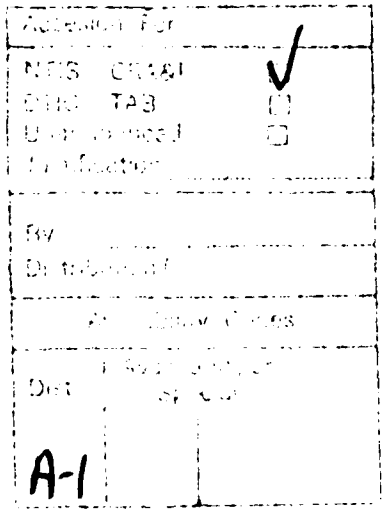

INTRODUCTION

In this report I have attempted to sort through the workings of a Synthetic-Aperture Radar (SAR). The motivation is to define those things which are based on physics and sorting out those which are engineering, which may have come to be considered basic to the SAR for whatever reason. The reason for this attempt was my ineptitude, in a discussion with an engineer who is new to the program to explain the motivation for such a program. The subject related to optical back-projection processing, which may find use in the processing of polar formatted SAR data. However, our discussions centered more on polar formatting and its whys than on optical back-projection and its attributes. This should be the real thrust of any optical back-projection program at this point. Application can come later!

I have felt for some time that descriptions of SAR have suffered from the same syndrome, i.e., topics which are really engineering conveniences have come to be treated as basics, and as such may impede attempts at alternates because of fear of the impact they may have on the SAR. The approach here is to define the SAR in terms of its most basic physical requirements and then explore the attributes of various existing implementations of these basics. Perhaps at some time in the future a reader of this report may ask, "That being the case, and if I don't violate the basic concept, what if...?" There is much that can still be done.

In the first sections of the report the basic physical principles of SAR are detailed. The radar is nothing more than an interferometer, with multiwave length capability, which can be used to measure the optical path lengths (optical path differences) to scatter points in the radar's field of view. Data on the target field is collected from various aspects. The composite of optical path data may then be considered as a whole and we have shown that is is ideally processed with a matched-filter. The physical attributes of the ideally matched-filter provide the basic limit of the radar's performance. The remaining sections of the report roughly follow the historical developments of SAR, and as we shall see, are based on engineering approaches taken to implement the desired matched-filter, and are not basic radar principles. One section relates the synthetic array to its real array analog.

The data of the earliest SARs were processed, using optical techniques after the data were literally arrayed in a range-azimuth format. A reader may more typically see this referred to as a range-doppler format. I avoid this designation as a Doppler shift is not a basic requirement of SAR. The characteristics of an optical processing implementation and its digital counterpart are detailed, and formatting-based physical limitations are described in a section entitled Processing Considerations. The drive for improved resolution lead to the intermixed (range-azimuth) matched-filter approach exemplified by polar formatting. A limiting form of the data formatted in this fashion is spatial frequency monotones which can be processed using Fourier-transform-like operations. Subsequent sections of the report center around techniques for the digital implementations of these Fourier-transform-like processes. The discrete Fourier-transform and the efficient FFT implementation are explained. Data interpolations necessary to allow use of the FFT algorithm are outlined. A final section deals with the general characteristics of back-projection processing. Its characteristics are illustrated by tying it back to the basic discrete Fourier-transform form.

The appendix illustrates digital processes which may be used to break the discrete Fourier-transform operation into smaller steps. Keep in mind that all the processing discussions pertain to various approaches to efficiently implement a matched filter and are not basic to SAR. However, the attributes of any one implementation may impact the performance of the radar implemented in this manner. Throughout the report, an attempt is made to estimate the digital computational complexity of the various matched-filter implementations.

To keep maximum emphasis of the basics, we have assumed a linear system so that the analysis can proceed by considering only a single-point target. We noted a need for the collection platform reference system and motion compensation, and they are ideal. Inphase and quadrative channels are needed to sort out ambiguous signals, as well as accommodate arbitrary scatter phases. We explored the characteristics of only one channel (both channels contain data with the same form). Finally, we ignored all the overhead functions which have to occur between the collection of the raw data and its appearance as a sample to a matched-filter emulator.

MICROWAVE INTERFEROMETRY

In this section, I will describe the hardware aspects of a Synthetic-Aperture Radar which I feel is its most basic physical form. All other descriptions can be derived from this basic form. This form is the radar which functions as an interferometer with multiple frequency capability. The radar collects data in the form of a differential phase between a received signal and a locally established and controlled reference. We will return to the reference form below. We will borrow from optical interferometry and refer to this differential phase as the optical-path difference since it involves line-of-sight distances to the target's positions.

If we assume that the radar operates in a linear region, we can view the received signal as the composite of returns from many scatter points in the radar's field of view. Thus, our interferometer will be simultaneously collecting the optical-path difference data for a large number of scatter positions. With this interferometer we can systematically collect the optical-path difference data for a band of frequencies and from different viewing aspects. The totality of data will contain optical-path data on each scatter point, but the history or variation in the optical-path difference with frequency and aspect will be unique for each target position. This uniqueness of optical-path difference history with frequency and aspect angle allows a single history to be sorted out from the jumble of signals available, i.e., detected. The precision of this sorting out process is limited by the bandwidth transmitted and the change in viewing aspect. Following sections of this report are devoted to various implementations which can be used in this sorting out process, starting with the ideal and its limits. The limits of the ideal processing scheme establish the basic limits of the physical process employed.

Before going on to the processing, go back to our basic radar and observe that we require not only coherency between the signal and reference at the time of any measurement, but an absolute coherence for the duration of the total observation. If the basic frequency of the radar is uncertain, an uncertainty in the optical-path difference histories and the sorting out capability may be negated, or at best be in error or ambiguous. This absolute coherency is established by tying the transmitter to the local oscillator, and the phasings of any modulations on each, to a local "absolutely" coherent source.

The reference for the interferometer is the radar's local oscillator, in our case, and its phase can be controlled to provide data with a structure consistent with a chosen processing scheme. We will return to some of these processing forms below. For now we can assume the local oscillator is locked to the coherent source with the consequence that the interferometer is measuring the total phase in the two-way path between the measurement position and the various scatter points. With the interferometer measuring the two-way optical path, it becomes necessary to have an instantaneous knowledge of the measurement position as the various frequency and angle measurements are made. If this is not the case, deviations in measurement position data (absolute path-length change) would be superimposed on the desired data, and separation may be impossible. The ideal of no relative-range change may be measurements at constant range and depression angle while viewing at various aspects, i.e., a constant altitude on a conical surface with its apex in the target area. The turntable SAR emulator is such an implementation. In practice, it is rather impractical to move on such a conical surface. Thus, we provided an inertial reference system as part of the radar's hardware implementation. This reference system is used to provide an instantaneous knowledge of the measurement platforms position. Inertially derived position data may then be used to alter the measured data so that it appears to have been measured at some other position, i.e., constant ranges on a conical surface with its apex in target space. It should be obvious that this modification (addition or subtraction of phase to the measured optical-path difference) also requires a coherent system.

The hardware described above is the totality of those necessary to implement a Synthetic-Aperture Radar. A coherent standard is required as is a position-sensing system if an absolute measurement position cannot be assured. The standard is ideally coherent over a time long, relative to the total measurement time. The position-sensing apparatus accuracy must be some small fraction of the operating wavelength.

There is no requirement for Doppler, nor is there any restriction on the modulation format. The Doppler description probably arose because of the aircraft motion and its convenience in specification of a PRF. The PRF is a sampling requirement reflecting the rate of change of the optical paths with angle, which is directly relatable to aircraft velocity if this velocity is the source of the angular change. The synthetic-aperture data may be collected from a stationary platform

which moves in any manner between measurements. The waveform is immaterial so long as its frequency components can be referenced to the same frequency components of the local oscillator. To eliminate ambiguities, there is a requirement on sampling density in both angle and frequency.

MATCHED FILTERING

Synthetic-Aperture Radar is based on matched-filtering concepts but for a different reason than those used to formulate the matched-filtering. The optimization of signal-to-noise ratio occurs in SAR as in any use of matched-filtering, but its application in SAR is tied more to the properties of the signal produced by the filter. Any signal-to-noise enhancement is, at best, related to an individual resolution element. The signal-to-noise ratio may be used to estimate the performance of a radar against a target of reference cross section and as such can be used to estimate the required transmitter power. However, these S/N considerations are secondary and a matched-filter would probably be used to process SAR data even in the absence of noise. The rationale for these statements will be illustrated in the remaining paragraphs of this section. We can begin by looking at the properties of a matched-filter and its performance when working with the optical-path difference data generated by our coherent microwave interferometer.

The matched-filter concept was originally formulated to provide a linear filter for the maximization of the detected signal-to-noise ratio when a signal is buried in noise, the noise being characterized as samples from a wide-sense stationary random process [1]. The knowledge that a signal does exist removes the constraint of preserving the signal form. Under the assumption of white noise (a flat power-density spectrum), an optimum filter has an impulse response form

$$h(\tau) = \frac{1}{N} S(t_1 - \tau), \quad 0 \leq \tau \leq T \tag{1}$$

where S(t) is the input signal and T is its extent. A filter with this characteristic is labelled a "matched-filter." It is obvious that the structure of S(t) has to be known to define the filter. The signal produced by such a filter is represented by the convolution integral

$$S_0(t) = \int_{-\infty}^{\infty} h(\tau)\, s\,(t-\tau)d\tau$$

$$= \frac{1}{N} \int_{-\infty}^{\infty} s(t_1-\tau)\, s(t-t_d - \tau)d\tau$$

where a time delay t_d has been included, i.e., a propagation path delay in the case of a radar or communications system.

The properties of a matched-filter can be illustrated by using (2) and letting $t_1 = t_d$, i.e., we seek some knowledge on the signal in the time slot where we may expect a signal. We should recognize that, in principle, we require a separate filter for each time slot of interest. This requirement is what drives us to look into a communications signal and provide huge amounts of processing for radar range compression. With $t_1 = t_d$ and the substitution $t' = t - t_d$ we find (2) taking the form

$$S_o(t') = \int_{-\infty}^{\infty} S(t_d - \tau)\, S(t' - \tau)\, d\tau$$

The above is the autocorrelation function for the signal referenced to the expected time delay. At $t' = t_d$, the indicated integration provides an output proportional to the energy in the signal (volts squared times time or current squared times time). Had we been in error in estimating t_1, the correlation time would shift in time by the estimation error. We also know the autocorrelation function of the signal is related to its power spectral density by the Fourier-transform relationship [2]

$$R(\tau) = \int_{-\infty}^{\infty} S(\nu) e^{i2\pi\nu\tau}\, d\nu \qquad (3)$$

The variable ν may be hertz or inverse distance. Drawing upon transform properties and considering a fairly uniform power density spectrum, note that $R(\tau)$ and/or $S(t')$ will display significant values only during a time interval of extent $1/B$ centered on $t' = 0$, i.e., about $t = t_d$. This time/space interval will contain most of the energy contained in the original signal. The amount of energy remaining in near-by time/space positions are side lobe levels and of concern when wide dynamic ranges are dictated. However, these sidelobes are not basic to an understanding of SAR and for purposes of illustration we can assume that our filter compresses all the incident signal energy into a time/space interval of extent $1/B$, where B is the bandwidth of the incident signal.

Considering an input signal of fairly uniform power we may represent the input signal-to-noise ratio as

$$\left(\frac{S}{N}\right)_i = \frac{S^2}{NB} \qquad (5)$$

We require a minimum bandwidth of B to pass the input signal. In the correlation time window the output signal-to-noise ratio becomes

$$\left(\frac{S}{N}\right)_o = \frac{(S^2\tau)\ (1/B)}{NB} = \left(\frac{S}{N}\right)_i \tau B \qquad (6)$$

The noise power is uncorrelated and remains uniformly spread over the interval T whereas the signal energy is compressed into a single time window of extent (1/B). This gain in signal-to-noise ratio in this time slot comes at the expense of the signal-to-noise ratio at all other times in the original signal extent T. While this is of no consequence for detection, it is unacceptable if the original signal structure has to be preserved. For the purposes of SAR we only need to note that a properly designed matched-filter compresses a signal of extent T into one of extent 1/B , i.e., a compression equal to the time/space-bandwidth product of the signal. The time-bandwidth product of a monochromatic pulse of length T approximates 1 and no compression is possible.

Let us now adapt the above to this microwave interferometer we call a SAR. We can invoke our linear system arguments and consider the signal generated by a single frequency at a single aspect. This signal is, in general, complex and may be represented with the phasor form

$$S = A\, e^{i(\phi - \phi_o)} \qquad (7)$$

where ϕ is the optical path length including array scattering phase and ϕ_o is the reference phase. To avoid tracking in-phase and quadrative channels let us assume a scattering phase of zero and work with only the in-phase channel. We note, however, that in any implementation we will require both in-phase and quadrative channels with identical forms. The matched-filter for a signal with the

form of (7) is approximated by the complex conjugate of the signal. Our processing is the detection of a signal from a particular point in radar space, with the signal buried in a composite of signals of the same complex form. We merely weight the composite of each measurement with the complex conjugate of (7), record the value, and then sum the results achieved when the same weighting is applied to all measurements. Each scatter point will have its unique matched filter.

To illustrate the azimuth resolution of a SAR we can consider we are gathering data on the returns from a point P, as a single frequency measurement system takes various positions along a straight line such as shown in Figure 1. In the case of an actual radar we will motion compensate the data to make it appear as though it had been collected while the aircraft was flying along a straight line. Our interferometer is measuring the optical path ν with the signal of interest approximating

$$S = Ae^{-2kr} = Ae^{\frac{-i2\omega r}{c}} \tag{9}$$

here $\nu = (R^2 + x^2)^{\frac{1}{2}}$, w is the radar radian frequency $2\pi\nu$, and c is the velocity of light in medium of interest. The spatial frequency of this signal at any position along the collection aperture is

$$\nu_s = \frac{1}{2\pi}\frac{\partial\phi}{\partial\nu} = -2\frac{\nu}{c}\frac{x}{(X^2 + R^2)^{1/2}}$$

$$= -\frac{2\nu}{c}\sin\theta \text{ radians/meter} \tag{10}$$

For small θ we see that the spatial frequencies are a fairly uniform function of θ, i.e., have a fairly uniform power density spectrum. In an interval $\Delta\theta$ as shown in Figure 1, we will observe spatial frequencies in the range

$$\frac{-2\nu}{c}\sin\theta_H \frac{\text{radians}}{\text{m}} < \nu_s \leq \frac{2\nu}{c}\sin\theta_H \frac{\text{radians}}{\text{m}} \tag{11}$$

With a matched filter we can then anticipate an isolation of the signal source to a position uncertainty (azimuth resolution)

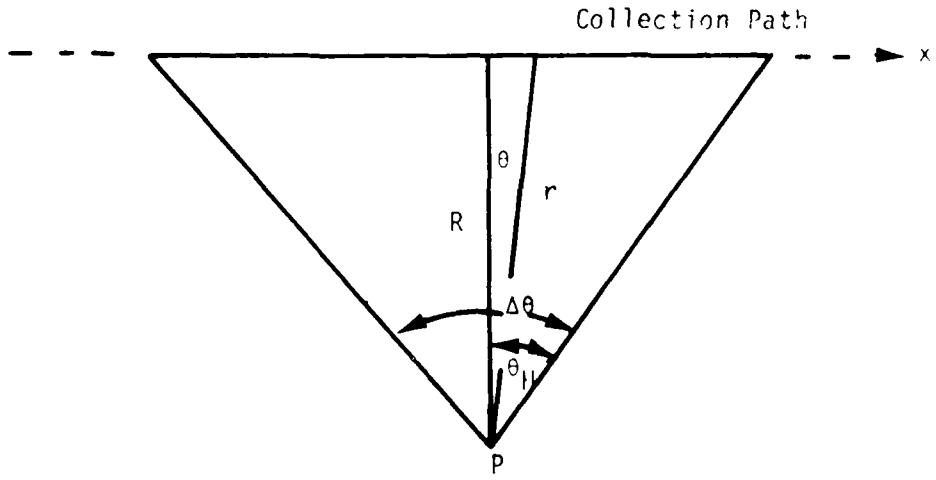

Figure 1. Elemental Synthetic-Aperture Data Collection Geometry

$$\Delta x = \delta_x = \frac{1}{B} = \frac{c}{4\nu \sin \theta_H} \text{ meters} \quad (11)$$

If we now consider $c = \nu\lambda$ the above becomes

$$\delta_a = \frac{(\lambda/2)}{2 \sin \theta_H} = \frac{0.5\lambda}{2\ (N.A.)} \text{ meters} \quad (12)$$

and about what we would expect for a lens operating at a wavelength with a numerical aperture of $\sin \theta_H$ [3]. The differences between (12) and the expressions of optics are the factor 2 because we are dealing with a two-way path, and a multiplier which reflects half-power points of the correlation function and not the square response we have assumed here. More familiar in the radar arena is the small-angle approximation of (12)

$$\delta_a \approx \frac{\lambda/2}{2\Theta_H} = \frac{\lambda}{2\Delta\Theta} = \frac{\lambda}{2}\left(\frac{R}{L_{syn}}\right) \text{meters} \quad (13)$$

Both of the above forms should be quite familiar, but here they have been developed assuming nothing more than a monochromatic interferometer, a particular data collection format, and matched filter processing. The interferometer and the matched filter comprise the only physics of Synthetic-Aperture Radar. The major efforts on SAR deal with engineering aspects, such as those related to processing which will be outlined in the following sections. All we have to do is engineer these simple physical principles.

Just as we may process the data in the azimuth direction with a matched filter we may consider our interferometer to have a multifrequency bandwidth B_T and matched filter the optical-path difference returns at the time delay or range of interest. These returns may be compressed to a pulse of length

$$\Delta t = \frac{1}{B_T} \tag{14}$$

corresponding to a range resolution

$$\delta_r = \frac{c\Delta T}{2} = \frac{c}{2B_T} \text{ meters} \tag{15}$$

In practice, we will have compressed the transmitted pulse T into a signal of extent Δt, or achieved a compression of

$$C_{omp} = \frac{T}{\Delta t} = T_{B_T} \tag{16}$$

equal to the time-bandwidth product of the transmitted signal. The returns of each PRF line must be compressed.

The item of note in this section is that the processing of our optical- path difference interferometer data can be accomplished using a matched filter if signal detection and relative signal strength data are the only requirements. The radar's performance is determined by the temporal bandwidth of the transmitted waveform and the spatial bandwidth of the azimuth or aspect data. The time/space data are compressed from their measured extents by their time/space bandwidth products during the matched filter process. If the frequencies to be processed are centered about zero, as in (10), we are in a minimal sampling requirement format and find the need for a minimal number of samples equal to the time/space bandwidth product of the signal of interest.

PHYSICAL ARRAY EMULATOR

The preceding discussion deals with the after-the-fact processing of data collected by a coherent measurement system. However, the processes have an analog in the form of a real array, as a real array can be built which will yield the same results. In this case the physical location of each element would be known. It need not be on a plane, but we will assume the elements don't block one another.

Considering the array as a whole, we want the energy from all elements of the array to arrive at a resolution element in-phase (constructive interference of the multibeam interferometer). Each element will transmit an identical waveform which provides the desired range resolution. The desired overlapping is accomplished by providing the desired waveform at each element and then adjusting its phase and/or time delay, relative to a local reference, to offset the path delay kr (modulo - 2π) or relative time delay to a given resolution element. This energy is scattered from the target and returned to the individual elements of the array. Upon reception, the signal at each element must again be adjusted in phase or time before it will constructively interfere with the returns collected by all other elements and provide us with the full array performance. To probe some other resolution element we appropriately readjust our phasing and/or timing at each element and repeat the process and continue in this manner until we have interrogated the space of interest.

In the SAR we have removed the time coincidence restriction and have combined the two phase/time operations into one. Other than that it should be apparent that the brute-force matched-filter SAR is an analog of a phased array with its elements positioned at the measurement points of the SAR. Both are interferometers. The real array is a real-time multibeam interferometer and the SAR, indirectly, is a multibeam interferometer by virtue of its coherent standard for all measurements.

PROCESSING CONSIDERATIONS

The preceding discussion deals with a single point in the field of view of the radar antenna. In practice, we are interested in all potential target positions in a neighborhood of P as illustrated in Figure 2. We can reasonably assume that we can adjust our antenna pattern so as to view all points in the area $D_r \times D_A$ (range and azimuth) as the synthetic-aperture length, L_{syn}, is traversed. Thus, our interferometer will collect data on all points in the target field of interest during its travel through the distance L_{syn}. We will now process these signals to determine the cross sections of a target at each of the positions in the neighborhood of interest. To avoid considering all targets, we assume a linear system and consider only a single target which is arbitrarily positioned in the field of interest.

We begin by assuming a brute-force processing of the data with a range compression factor $T B_T$. Thus, we will require at least $T B_T$ complex operations (multiply plus add for the minimum of TB samples) to compress the range data for a given resolution element for each PRF line. We require a minimum of LB_A PRF lines or a minimum of

$$(TB_T)\ (L_{syn}\ B_A) \tag{17}$$

operations just to process the range component of a given resolution element. In addition, we require a minimum of (LB_A) operations on the data <u>after</u> it has been compressed in range to accomplish the azimuth compression for a given resolution element. Considering that we have

$$\left(\frac{D_a}{\delta_a}\right)\left(\frac{D_r}{\delta_r}\right)$$

resolution elements in the field of view of interest we arrive at the minimal number of operations per channel required to produce the desired image,

$$(LB_A + (TB_T)\ (LB_A))\ \frac{D_r}{\delta_r}\ \frac{D_a}{\delta_a}$$

If we assume $TB_T \gg 1$ and use (11) and (13), the above may be approximated as

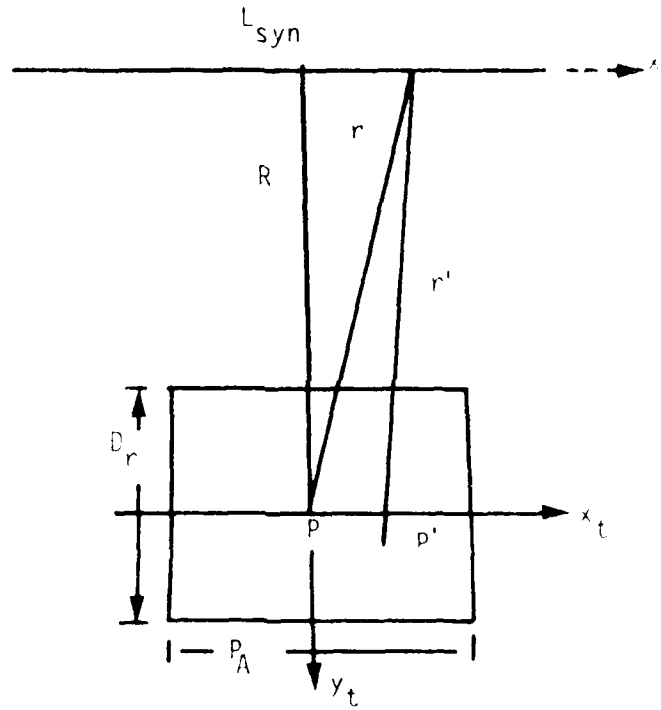

Figure 2. SAR Data Collection Neighborhood

$$\left(\frac{\lambda R}{2\delta_a^2}\right)\left(T\,B_T\right)\left(\frac{D_r}{\delta_r}\right)\left(\frac{D_a}{\delta_a}\right) \tag{20}$$

required operations per channel (range processing clearly dominates). The numbers became rather large for practical radar values, and has been fought for years. If, in addition, we impose the continuous strip map condition

$$D_a \geq L_{syn} \tag{21}$$

we arrive at an approximate requirement for

$$\left(\frac{\lambda R}{2\delta_a}\right)^2 \left(T\,B_T\right)\left(\frac{D_r}{\delta_r}\right) \tag{22}$$

operations per channel per image.

Consider the following radar example:

$$\begin{aligned} R &= 0.5 \times 10^5 \text{ meters} \\ \lambda &= 3 \text{ cm} \\ \delta_r &= 1 \text{ m} \\ \delta_a &= 1.5 \text{ m} \\ D_r &= 10^4 \text{ m} \\ TB_T &= 2 \end{aligned} \tag{23}$$

We would require approximately 10^{11} operations per channel to produce an image of an area of $(10^3) \times (10^4)$ meters squared. The minimal synthetic- aperture length would be 1000 meters or about 5 seconds for a platform velocity of 200 m/sec (~ 0.7M). Thus, we see a basic minimal single-channel processing requirement in excess of 10^{10} operations per second for a real-time strip map.

Processors for synthetic aperture radar data have evolved along the line of sequential range and azimuth processing. Part of this may be optically driven.

However, we can see a rationale for this by considering the matched filter for the point P' illustrated in Figure 2. The point is assumed to be in the field of interest and its ideal matched filter would have the form

$$e^{-i\phi(r')} = e^{i2kr'} \tag{24}$$

for the signal form

$$A(r')\, e^{-i2kr'} \tag{25}$$

collected along the data collection path. Looking at the filter form, we note that mathematically we may represent r' as

$$r' = r'\Big|_{r_o} + \frac{\partial r}{\partial x_t}\Big|_{r_o} x_t + \frac{\partial r}{\partial y_t}\Big|_{r_o} y_t + \ldots \tag{26}$$

where r_o is the distance to a reference point in the radar's field of interest. If the higher order terms can be ignored, the matched filter for off-reference-position points in the radars field car be viewed as linear, target position dependent, and perturbations from the matched filter for the reference point. What this implies is that the processing can proceed by first filtering all data along L_{syn} using the matched filter for the reference point. The residual data can then be processed in some manner to sort out the desired information for the other points in the neighborhood of the reference point. We will look at some historical implementations below, but let's first look at some general limitations of the implied range-azimuth processing.

Considering range and cross-range coordinates, we see a signal from a - μ aspect, as in Figure 3, would have a matched filter form approximating

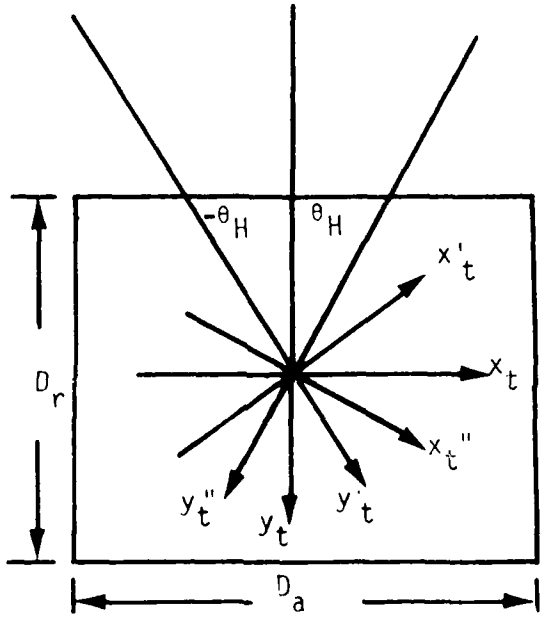

Figure 3. Aspect Angle Change of Range and Cross Range Distances

$$r'(-\theta_H) \simeq r + \frac{\partial r'}{\partial x_{t'}}\bigg|_r x_t' + \frac{\partial r'}{\partial y_{t'}}\bigg|_r y_{t'} + \ldots \quad (27)$$

From $+\theta_H$ the form would approximate

$$r'(\theta_H) \simeq r + \frac{\partial r'}{\partial x_{t''}}\bigg|_r x_t'' + \frac{\partial r'}{\partial y_{t''}}\bigg|_r y_t'' + \ldots \quad (28)$$

As pointed out by Brown and Fredricks [4] the residue phase can be processed in a range-azimuth (rectangular) sequence so long as the x_t' and x_t'' representing a target position X_t deviates by no more than one-half a resolution element as viewed from various aspects. Likewise for y_t' and y_t''. The most change occurs at the edges of the field, and for a given $\Delta\theta$ we can impose the field-of-view limitations

$$\frac{D_r}{2}\,\Delta\theta < \delta_a \quad (29)$$

and

$$\left(\frac{D_a}{2}\right)\Delta\theta < \delta_r \quad (30)$$

Using (13), the above become the expressions of Brown and Fredricks [4],

$$\delta_a^2 > \frac{\lambda D_r}{4} \quad (31)$$

and

$$\delta_r \delta_a > \frac{\lambda D_a}{4} \quad (32)$$

Returning to our consideration of sequential range-azimuth processing, i.e., we first process the returns in range, and array the data into range bins for subsequent azimuth processing. This involves compressing the returns with a matched filter for each range bin or

$$(TB_T) \quad (\frac{D_r}{\delta_r}) \tag{33}$$

operations per PRF for a range swath of D_r . This range processing may also be accomplished in an analog fashion with a dispersive delay line operating on chirp signal, a tapped delay line for other signal forms, etc. Under this condition we may treat Dr as δ_r and (31) becomes

$$\delta_a^2 > \frac{\lambda \delta_r}{4} \tag{34}$$

and a not too stringent requirement for reasonable resolutions. However, if we look at (32) and impose the strip map requirement $D_a \geq L_{syn}$ we arrive at

$$\delta_r \delta_a > \frac{\lambda D_a}{4} > \frac{\lambda L_{syn}}{4} = \frac{\lambda^2 R}{8\delta_a} \tag{35}$$

or

$$\delta_a^2 \delta_r \geq \frac{\lambda^2 R}{8} \tag{36}$$

This latter condition can easily impose resolution values in the meter range for the assumed sequential range-azimuth scheme of processing. We can contrast this to an ideal point-by-point matched filter where we may only limit the half angle to perhaps 30° (because range and azimuth data provide the same resolution characteristic at 90°) and can obtain limiting resolutions on the order of λ . We need not concern ourselves with the whys of the above limitations as we will later look at procedures to overcome them. They can be explained in a number of ways. For now let us look at how processing has evolved.

Radar data was initially processed optically by recording data on film in a scaled range-azimuth format. Optical processing allows compression of wideband chirp signals with good range resolution and with azimuth resolutions on the order of those indicated in the above illustration. The most successful processings have been those made with the data formatted for the tilted plane processor [5]. While optical processing has many nuances let us leave it at this point and go back to our description of the data form and the digital processing implications. We will return to a discussion of optical processing later when we make use of the 2-D Fourier-transform property of a lens.

Let us consider here the data contained in a range bin of extent ℓ_r as illustrated in Figure 4. We simultaneously collect the data for all target positions in this range bin along the synthetic-aperture length L_{syn}.
The matched filter for an arbitrary point x_t in this limited field is

$$e^{i2kr'} \tag{37}$$

where

$$r' = [R^2 + (x-x_t)^2]^{1/2} \tag{38}$$

Expanding r' in a Taylor series about $X_t = 0$ we have

$$r' \approx r + \frac{\partial r'}{\partial x_t}\bigg|_{x_{t=0}} x_t = r - \frac{xx_t}{r} \tag{39}$$

The matched filter for the point x_t approximates

$$e^{i2k\left[r - \frac{xx_t}{r}\right]} \tag{40}$$

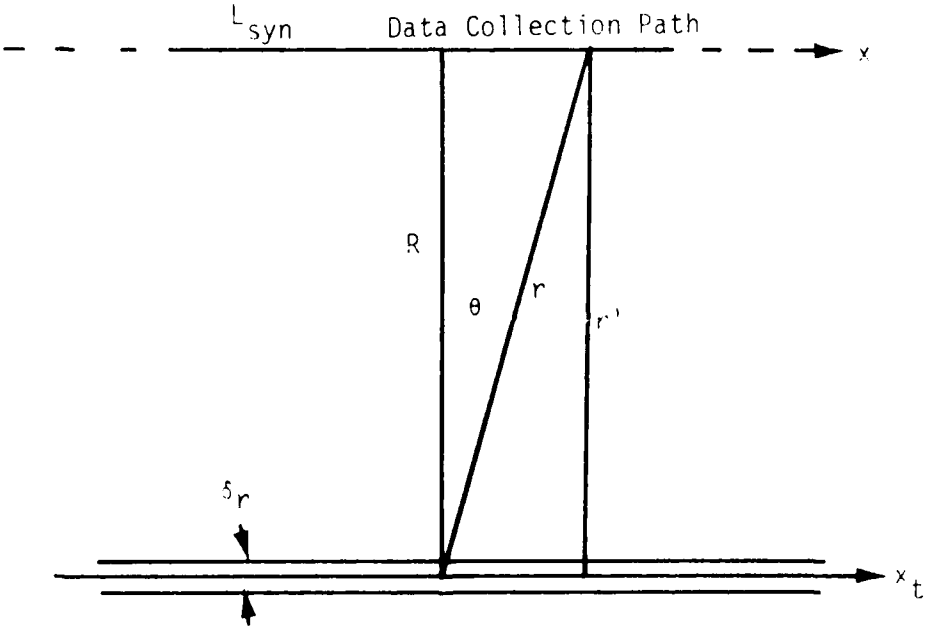

Figure 4. Single Range Bin Data Swath Width

Rather than implementing this filter for each X_t let us look at the phase residue after the matched filter function for the point $X_t = 0$ is removed from all data in the range bin. This operation leaves a residue

$$A_t \; e^{i2k\left(-\frac{xx_t}{r}\right)} \tag{41}$$

to be processed. Note that sampling considerations have not been explicitly addressed, but we assume sampling is adequate. The PRF (azimuth sampling) of the radar may be affected by the particular hardware implementation selected, as will things like presuming during data processing. Here we are addressing the minimal processing requirements of some optimal data collecting implementation.

If we look at (41) we see the residual signal retains a bandwidth of

$$B_{res} = 2\left(\frac{1}{2\pi}\left.\frac{\partial\phi}{\partial x}\right|_{x_{max}}\right) = 2\left(\frac{L_{syn}}{\lambda\, r_o}\right) = \frac{1}{\delta_a} \quad \frac{\text{radians}}{\text{m}} \tag{42}$$

for $X_{max} = L_{syn}/2$. This implies (L_{syn}/δ_a) samples and processing operations for each of the (L_{syn}/δ_a) azimuth resolution elements in the range bin of interest. These operations come on top of the operations required to remove the reference point matched filter from the data. The reference point variation can be removed in the analog portion of the radar. Digital removal of the central matched filter implies (continuous strip format)

$$\left(\frac{L}{\delta_a}\right) + \left(\frac{L}{\delta_a}\right)^2 \tag{43}$$

operations to process the azimuth data in each range cell. These azimuth operations are in addition to the

$$\left(T\, B_T\right)\left(\frac{L}{\delta_a}\right) \tag{44}$$

operations required to assign the data to appropriate range bin. The minimal number of operations for our channel strip map for this case being

(Operations/range bin) x (# of range bins)

$$\left(1 + \frac{L}{\delta_a} + TB_T\right)\left(\frac{L}{\delta_a}\right)\left(\frac{D_r}{\delta_r}\right) \tag{45}$$

The form is different from that for the brute-force case as are the number of operations. For our radar example given above, L_{syn}/δ_a will dominate TB_T, and the range-processing requirements become insignificant relative to azimuth processing, with the result that we now minimally require approximately

$$\left(\frac{L}{\delta_a}\right)^2\left(\frac{D_r}{\delta_a}\right) \tag{46}$$

operations. We have actually increased the required number of azimuth-related operation, but have reduced the required number of range operations by treating (L/δ_a) azimuth elements as though they have the same range filter, i.e., always lie in a single range bin. The original brute-force example, a direct implementation of the mathematical matched filter, assumed <u>each</u> resolution element required its unique range matched filter. With the azimuth processing a dominate factor, we can conceptually explore reducing this load more.

If we return to (41), we see that for small θ (r a weak function of x) the residue function for a signal in a given range bin takes the approximate form

$$A_t\, e^{\,i2k\,\frac{xx_t}{R}} \tag{47}$$

where R is the broadside range to the target in Figure 4 It may be a mean target range for other squint angles. The residual signal approximates a constant spatial frequency with the frequency proportional to the target position X_t. The desired processing is a spectral analysis which can be performed batchwise using an FFT

algorithm. The FFT will be addressed in more detail below. It is expedient to reduce the required number of azimuth operations to the order of

$$\left(\frac{L}{\delta_a}\right)\log_2\left(\frac{L}{\delta_a}\right) \tag{42}$$

The FFT implies (L/δ_a) is an integer power of 2, and is some value so that it spans the azimuth swath width D_A. The number of azimuth operations

$$\left(\frac{L}{\delta_a}\right)^2 \tag{43}$$

given by (43) would be the required number for a brute-force matched filter approach. The Fourier-transform operation requires a like number if an FFT algorithm is not employed. Processed with a FFT algorithm the required per channel operations now approximates

$$\left(1 + \log_2\left(\frac{L}{\delta_a}\right) + TB_T\right)\left(\frac{L}{\delta_a}\right)\left(\frac{D_r}{\delta_r}\right) \tag{50}$$

and range compression may dominate once more.

The above illustrated an efficiency offered the azimuth processing when a common factor is removed from all data in a range bin leaving an azimuth data residue which can be processed with an efficient algorithm. A similar efficiency for the range data may be postulated if the range data were in a form which could be processed by spectral analysis. This is the data form produced when the "Stretch" technique described by Capati [6] is employed.

The chirped return from a target point at range r'

$$s_t \sim i2\pi\left[\nu_0\left(t - \frac{2r'}{c}\right) + \frac{1}{2}\left(t - \frac{2r'}{c}\right)^2\right] \tag{51}$$

is mixed with a reference signal form

$$e^{i2\pi[\nu_0 (t - \frac{2r}{c}) + \frac{1}{2} (t - \frac{2r}{c})^2]} \qquad (52)$$

rather than the fixed frequency reference implied in all previous illustrations. The result is a monotone video signal whose frequency is dependent on the differential range (r'-r). This signal has the parametric frequency form

$$\nu_{video} = \frac{2}{c} (r' - r) \text{ hertz}$$

The transmitted B_T is T and a resolution $c/2B_T$ can be produced. The processing of these signals is a spectral analysis and an FFT may be employed. We are now considering the data from more than one range bin and the range swath imposed limitation (31) may come back into play. Brown and Fredricks were working with such chirped signals and the rotary table SAR emulator at the Willow Run Laboratories (now ERIM) when their paper, referenced above, was published.

While we may, on the surface, now anticipate more reduction in our processing load, the range data structured as above and implemented with an FFT requires some tradeoffs. We recall each PRF required

$$\left(TB_T\right)\left(\frac{D_r}{\epsilon_r}\right)$$

brute force range processing operations to compress the data and assign it to one of (D_r / ϵ_r) range bins. We operated under a swath-width constraint with the form

$$a^2 > \frac{1}{4} D_r$$

and were quite happy. Processing this modified range data with a brute-force Fourier-transform will require the same number of operations. However, we would like to exploit the FFT algorithm's efficiency in our spectral analysis. This comes at a price.

The TB product of the input signal dictates the minimal size of our FFT. In the example above we assumed 20 for a TB product. We could implement a 32-point FFT and pad with zeros. The processing would separate data into 32 one-meter range bins. This 32-meter swath applied to (31) does not impact our desired 1.5m azimuth resolution. The problem is that we have been forced to consider only a narrow range swath when low TB products are employed. For our model radar we would have to employ 10^4 TB) separate L.O.'s, with each representing an appropriate range dela.. However, let's proceed and note that we now require

$$TB_T \log_2 (TB_T) \tag{32}$$

range processing operations for each of subswaths of width (TB_T) . For each FFT we would require

$$\log_2 (TB_T) \left(\frac{D_r}{\delta_r}\right) \tag{33}$$

operations. A rather curious result says that the processing load goes down as we decrease the TB product. We do indeed reduce the processing burden to the limit of a short pulse, $(TB_T) = 1$. However, we have shifted the burden to an extremely complex r-f section that probably could not be implemented.

If we take the tack of minimal L.O.'s in the above, we find (31) limits us to a sub-swath width given by (example numbers assumed)

$$1.5^m \cdot \left(\quad\right) \text{(sub-swath width)} \tag{34}$$

For the example values this would be about 167 meters. Let us select TB = 128, and consequently, a subswath of 128 meters for the assumed range resolution. We would require about 80 local oscillators and

$$\log_2 (12g)\left(\frac{D_r}{\delta_r}\right) = 7\,\frac{D_r}{\delta_r}$$

range processing operations. This number is not a lot different from the brute-force $20\,(D_r/\delta_r)$ indicated for the brute-force processing of an arbitrary $TB_T = 20$ signal, assumed above. This small improvement comes at the expense of a severe implementation penalty.

The above would seem to indicate that for moderate resolutions, the separation of data into range bins for subsequent azimuth processing can afford significant processing efficiencies over the brute-force approach to the ideal matched filter operation. The azimuth signals in a given range bin can, in general, be additionally formatted and batch-processed using an efficient algorithm to affect even greater overall processing efficiency. However, a formatting of the range data into a similar form for batch processing provided, at best, mixed results. We did not observe these mixed results in the azimuth processing since they were not anticipated, and the space bandwidth product processed was only that required to produce the desired map rate, i.e., a real-time strip map. While we may consider breaking the azimuth into small batches, Appendix A shows that this does not reduce the digital processing load. There is a large overhead in the formatting operation which was not visible in the range example given above as the complexity was forced back into the hardware.

2.2.2 FORMATTING OF RADAR DATA

The polar formatting of radar data was conceived by Walker [3] in response to the limitations described by Brown and Fredricks [4] during their efforts with the first generation of the motion platform SAR emulator. In this section, we will present the basic physical basis for the concept, and not a particular implementation. We feel that the observations of Walker are quite elegant and the physical picture is greatly obscured with the introduction of the chirp waveform and Doppler frequency in the basic description of the concept. The chirp waveform provides a convenient implementation approach, but is not basic to the concept. Some additional comments on this point will be provided later in this section.

To develop the basis of the polar format, consider the target referenced data collection geometry illustrated in Figure 5. We assume that targets of interest are positioned in the neighborhood of the origin of an inertially defined (x_t, y_t) plane, and that data collection occurs from a remote inertially determined point P, which is normally not in the (x,y) plane. The observation point P and the z axis define a hypothetical collection plane which would intersect the (x_t, y_t) plane as shown. This intersect makes an angle θ with the y_t axis. The line-of-sight distance from the observation point P to the reference point is denoted as r_0, and intersects the (x_t, y_t) plane at an instantaneous observation depression angle ψ. The line-of-sight distance from P to an arbitrary target position (x_t, y_t) is denoted by r.

We apologize for what may seem a weird and unconventional selection of coordinate designations, i.e., a left-handed basis system. However, there is a method to this which becomes more evident as we discuss image forms below. For now we will assume a motion platform with nominal movement in the x_t direction, i.e., antenna on the right-hand side of collection vehicle. Using the coordinates shown, the image produced will be one which would correspond to what an observer would see looking out the right-hand side of collection platform. On a display, range may be in the vertical direction, with far ranges at the top of the display, and the positive x_t direction on the observer's left. In a strip map mode, the image would move to the right across the display as time proceeds. In the same manner, the radar space would be by an observer on the collection platform.

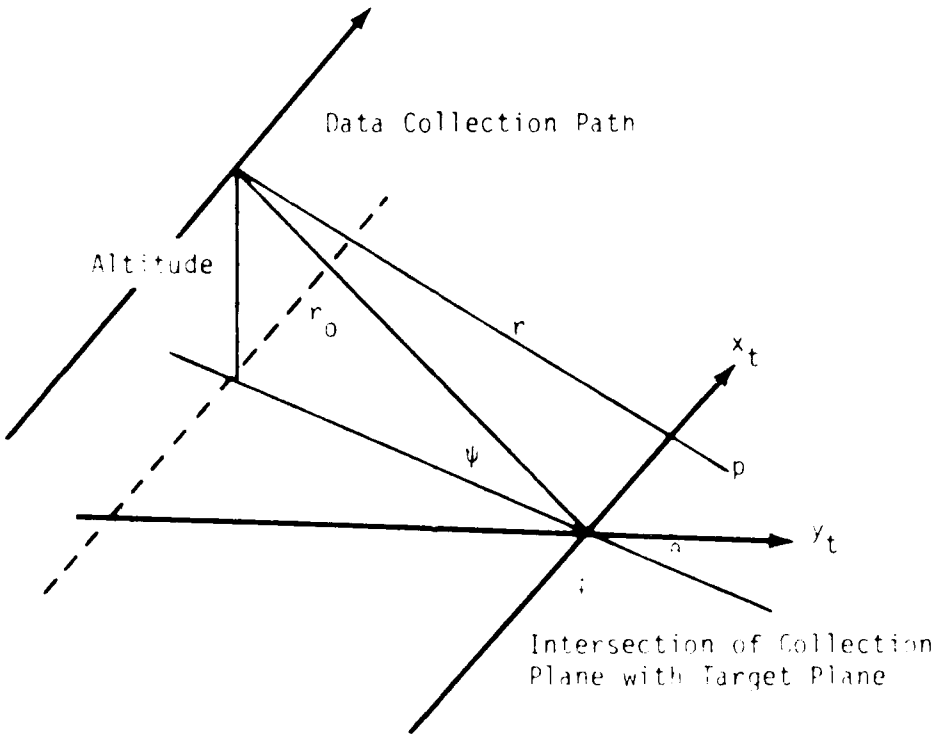

Figure 5. Data Collection Geometry Used for Spotlight

The simple elegance and power of polar formatting can be [illegible] the data collection system as an interferometer with frequency [illegible] the coherence properties of an interferometer is the [illegible] needed to implement the radar. While perhaps capable [illegible] frequency transitions [illegible] invoke our linear system [illegible]

[illegible] is using a [illegible] series of monotones, with each [illegible] [illegible] to provide an adequate signal-to-noise ratio. The [illegible] interferometer [illegible] of the transmitted monotone [illegible] [illegible] to a range [illegible], i.e., the return [illegible] [illegible] [illegible], received using our [illegible]

[illegible]

[illegible] we will receive a return with the form

$$[illegible]$$

[illegible] these as we are doing here. This signal is compared to the [illegible]

$$[illegible]$$

[illegible] comparison is an optical-path difference of [illegible]

$$[illegible]$$

[illegible] the optical-path difference between [illegible] [illegible] the rate of change of the optical-path difference, will [illegible] frequency, as [illegible] for [illegible] [illegible] band of frequencies, [illegible] [illegible] we move on to [illegible]

viewing aspect, i.e., different θ, and repeat our measurements. We have not required continuous motion nor a chirp. The only requirements are a knowledge of r_o, , and, as we will illustrate shortly, the angle θ associated with each observation.

The reference process outlined above is the removal of the optical-path data representative of the point r_o from the composite of data collected. We have removed the matched-filter data for point (0,0) from all data. For other scatterers in the field of interest, we are left with a phase residue which is dependent on , , , x_t and y_t. Let us attempt to characterize this residue.

Expressing r as a function of r_o and the various parameters we find

$$r = [(r_o \sin \quad)^2 + (r_o \cos \psi \sin \theta - \psi_t)^2 + (r_o \cos \psi \cos \quad + y_t)^2]^{1/2} \qquad (64)$$

Expanding r in a binomial series about r_o we find

$$r = r_o - x_t \cos \psi \sin \quad + y_t \cos \psi \cos \theta + \ldots \qquad (65)$$

and in the paraxial approximation limit

$$(\quad, \theta) \quad \frac{4\pi}{\lambda} (r - r_o) \quad \frac{4\pi}{\lambda} \nu [-\cos\psi \sin \theta x_t + \cos \psi \cos \theta \, y_t] \qquad (66)$$

As once stated by Walker [8]; "The form begged for polar representation." The basic polar parameters being and θ with the coordinate scaled by $\cos\psi$. In this illustration, the angle coordinate θ is not the conventional polar coordinate angle . We assume that the data space cartesian axes correspond to those of the radar space as illustrated in Figure 6. The data from any measurement made at angle is conceptually formatted along a radial line in this data space at a radius of . The radial line makes the same angle θ to the y data axis as the collection plane intersection made to the y_t radar space axis. The data space cartesian coordinates being related to , and by the transformation expressions

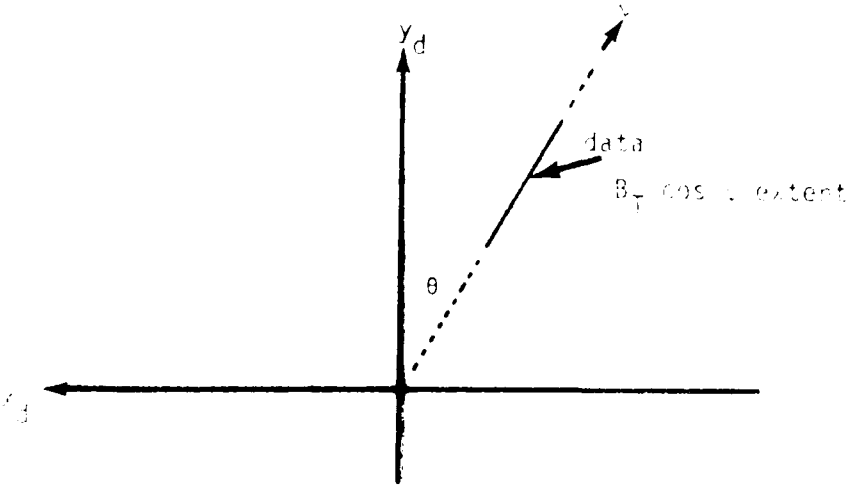

Figure 6. Conceptual Format of Residue Data in Modified Polar Coordinates

$$x_d = - \nu \cos \psi \sin \Theta \tag{67}$$

and

$$y_d = \nu \cos \psi \cos \Theta \tag{68}$$

We assume that the number of frequency samples along a data line, such as that illustrated in Figure 6, is adequate to unambiguously specify the phase of the various range cells of the radar space as viewed from that perspective. Moving to a new perspective will provide a new set of phases, and we also assume an adequate sampling in the θ direction to unambiguously specify the change between observation angles. If the measurements are made sequentially from a moving platform it should be obvious that θ changes and the data line will not be a radii in x_d, y_d space.

Proceeding with our frequency and angle sampling of the radar space, we could eventually (a week, a second, 10 microseconds) populate the data space in the neighborhood of ($\nu_0 \cos$, θ_0) with individual target data samples representative of continuous signal with an approximate form

$$A_t \, e^{i \frac{4\pi}{\lambda} [x_d x_t + y_d y_t]} \tag{69}$$

While perhaps not obvious, this formatting to first order, removes the data wander of Figure 3 which concerned Brown and Fredricks. However, range and azimuth have lost their distinct relationship to data axes. To extract the desired cross-section information, A_t, we may want to perform a 2-D spectral analysis as the approximate signal has the form of a 2-D spatial monotone. Each potential scatter position is represented by a unique 2-D spatial monotone. An efficient spectral analysis which will simultaneously extract data on all monotones of interest is a 2-D inverse Fourier-transform of the data in an extended aperture of the data space.

Because of the form of a 2-D inverse Fourier transform, we can translate our data

axis reference to the position, ($x_o \cos(\alpha_o)$, y_o), and incur no more than an immaterial constant phase offset. The processing aperture may now be viewed as that shown in Figure 7. In this aperture the data exists as samplings of the superposition of many 2-D monotones. The samplings having nominally occurred along offset center radial lines such as those indicated. While the sampling format comes into play in processing, we can view the signals as continuous and use Fourier-transform properties to provide a first-order description of the processed image characteristics. These descriptions will comprise the remainder of this section. Processing details will be considered in later sections.

We have assumed a linear system to this point and have dealt with an arbitrarily positioned target in some neighborhood of radar space. We have defined the first order characteristics of the residue signal which remains after its formatting in a particular fashion and have defined a processing scheme. Now is a convenient time to consider we do not have one signal of the form (69) in the data aperture but a composite with the form

$$\sum_j A_{tj} e^{i \frac{4\pi}{\lambda} [x_d x_{tj} + y_d y_{tj}]} \tag{70}$$

We can process this signal using the 2-D inverse Fourier transform with the result

$$S_o(x_i, y_i) \propto \int_{-\infty}^{\infty} \int_{-\infty}^{\infty} \left(\sum_j A_{tj} e^{\frac{i4\pi}{\lambda} [x_d x_{tj} + y_d y_{tj}]} \right) \cdot \left(e^{\frac{i4\pi}{\lambda} [x_d x_i + y_d y_i]} \right) dx_d \, dy_d \tag{71}$$

In the above x_i is aligned with x_d and y_i with y_d. Interchanging the orders of summation and intergration we quickly arrive at

$$S_o(x_i, y_i) = \sum_j A_{tj} e^{i\phi_j} \delta(x_i - x_{tj}, y_i - y_{tj}) \tag{72}$$

The signal magnitude at an image position (x_i, y_i) being proportional to the strength of the signal A_t scattered from the conjugate geometric position in radar space, i.e., we have an "image" or map of the scattered field amplitude.

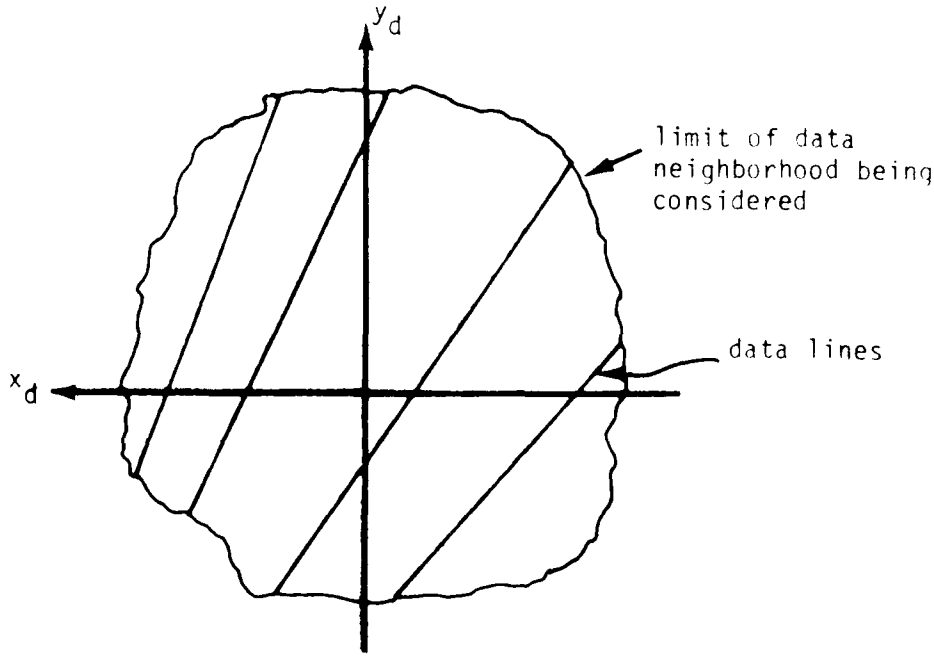

Figure 7. Data Lines Within Processing Aperture

In practice the image is not a series of delta functions, but has a resolution limited by a finite data aperture. This finite aperture leads to an image positional uncertainty

$$\Delta x_i = \Delta x_t = \frac{C}{2L(x_d)} \tag{74}$$

and

$$\Delta y_i = \Delta y_t = \frac{C}{2L(y_d)} \tag{75}$$

where $L(x_d)$ and $L(y_d)$ are the data extents in the orthogonal x_d and y_d data directions. If we consider the broadside case we have

$$\Delta y_t = \frac{C}{2B_T \cos \psi_o} \tag{75}$$

and

$$\Delta x_t = \frac{C}{2(\nu_o \cos \psi_o \Delta\theta)} \tag{76}$$

where B_T is the spread of frequencies employed, ψ_o is the broadside depression, ν_o is the center frequency and $\Delta\theta$ is the angular extent of the data considered. The y_t resolution is $(1/\cos \psi_o)$ worse than the $C/2B_T$ indicated previously for an ideal matched filter and is merely a reflection of the slant-range to ground-range relationship illustrated in Figure 8. The cross-range resolution is also scaled from the indicated matched filter resolution ($\lambda/2\Delta\theta$) by the same $(1/\cos \psi_o)$ factor. This may be somewhat confusing until we consider that the previous resolution, ($\lambda/2\Delta\theta$), involved the change in aspect in the collection space. The $\Delta\theta$ in (76) is a change in projected space. For this example, the collection platform

would have only viewed the target through an aspect of $\Delta\theta \cos \phi_0$ and our original matched filter guidelines remain inviolate. The data collection angle change is less than the formatted $\Delta\theta$ for any ϕ unequal to zero.

The above presented only a digital perspective for the processing of the data. We have conceptually formatted or arrayed the data for a large θ change in an annular-like strip such as that illustrated in Figure 9a. The discussion above centered upon the processing of a subaperture of this data with the processing axes aligned with the format axes as shown in Figure 9b. The result is an image with an (x, y) orientation corresponding to the broadside ($\theta = 0°$) view of the target. To a first order the image has a form which is insensitive to the actual portion of the total data record being processed. The data may also be processed against any other set of reference axis, for example as those of Figure 9c where the y_d axis is aligned along the ϕ_0 direction. In this case the image will have a perspective of the target area corresponding to the view from the nominal angle of the data collection. The choice of processing axis is basically not process dependent, and the choice may well be made for other considerations. Noncoherent addition of images to reduce speckle may indicate a preference for the nonrotating image produced by the orientation of Figure 9b. An image providing the observer a target perspective would be produced by the orientation of Figure 9c.

The above would seem to indicate that we have eliminated all our problems and can proceed to consider processing details. However, we should keep in mind a couple of caveats. The foremost is the actual structuring of the data into forms that are useful in our conventional transform implementations. This aspect will be addressed in the following sections. The second is that we have only dealt with the paraxial limit of the binomial expansion of r about r_0. In practical terms we have considered only the phase residue for points in the "near" neighborhood of the reference point after removal of the matched filter, r_0, from all data. Factors which can perturb the neatness of the above are contained in the higher order phase terms which were ignored. These factors contribute effects analogous to, but not one-to-one, the classical aberrations of optics. Distortion is analogous and is inherent in the terms of (65) which were ignored. The usual chirp spotlight implementation also introduces a distortion. While the chirp provides a convenient

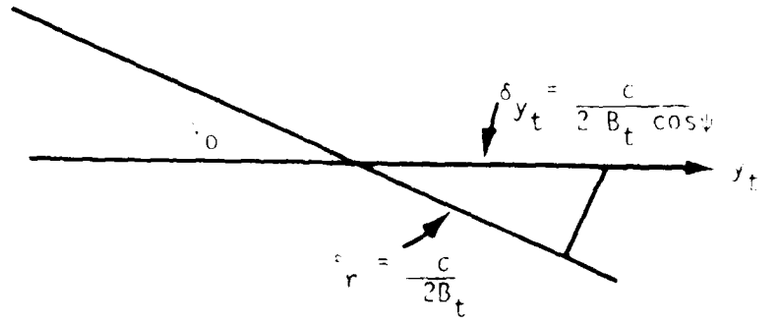

Figure 8. Slant-Range Ground-Range Relationship

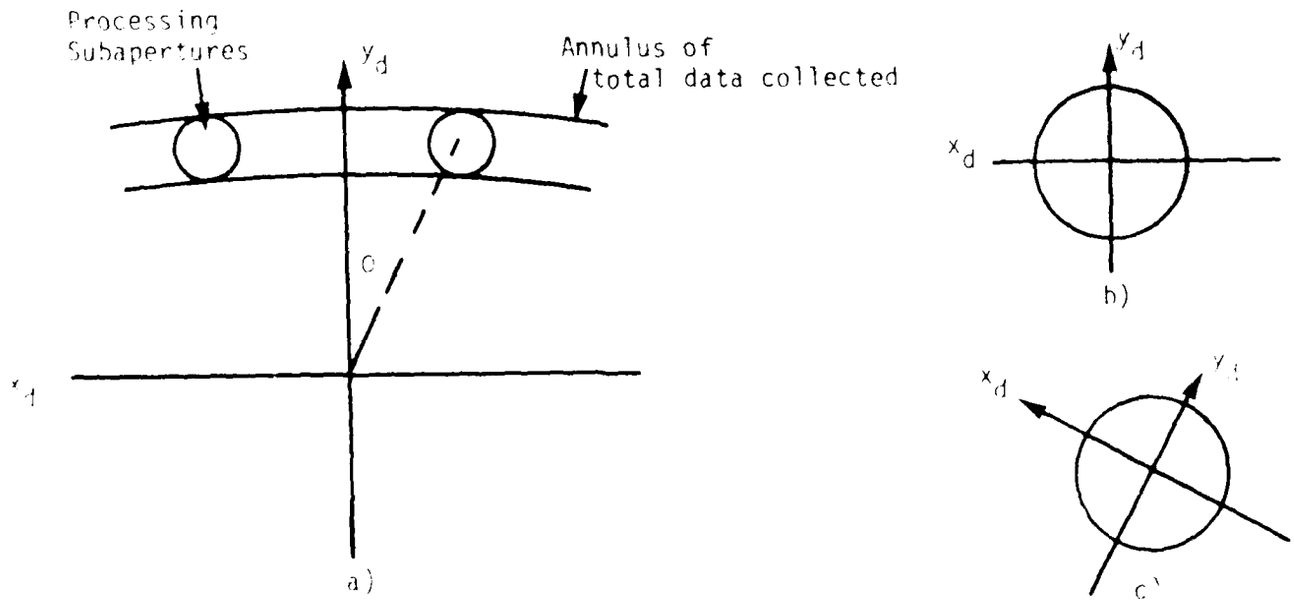

Figure 9. Collected Data Format and Axes Orientation Variations in Processing Step

means of scanning a bandwidth in a known and regular manner, it does disrupt our interferometry. The return from a point at range different from the reference point is offset from the reference frequency.

I have, in fits and starts, been attempting to sort out these effects for a number of years. The details are tedious and cumbersome, and as noted, the forms do not lend themselves to classical optical interpretations. However, I feel I am somewhat near and this report may serve as a prod to go back and attempt to generate some sort of report which at least summarizes activities to date, and at best may provide definitive insight into the influence of the ignored terms. The forms considered in this associated analysis will also allow for rapid evaluation of the influence of deviations from the ideal, i.e., velocity measurement errors, influence of formatting to aircraft angle rather than ground angle, etc.

OPTICAL PROCESSING

To this point we have dealt with the general collection and formatting of radar data into a form where it may be processed to produce an image of the scatter points of interest. The primary descriptions of processing have been digital based. This section is included to provide an introduction to optical processing. The polar formatted signal has taken a form which may be processed using a 2-D inverse Fourier transform. If the data are physically mapped onto a coherent 2-D spatial light modulator the signal phases will appear as 2-D phase variations on a nominally planar coherent optical wavefront. A simple lens will accomplish a 2-D Fourier transform and can be used to process this data from [9].

The traditionally optical processing of radar data has not been of a Fourier-tansform nature and a much more complex processor is involved. The spatial light modulator has traditionally been photographic film with the data arrayed in a range-azimuth format. A scaling in both range and azimuth is required to record the data on reasonable-sized film formats. For a typical azimuth signal, (38), we recall the phasor form (37) represents a real video signal

$$A_t \cos 2k \left[R^2 + (v - x_t)^2\right]^{1/2} \qquad (77)$$

This signal is amplified and used to expose a photographic film in a range bin somewhere across the films width. The exposure is adjusted so that the processed film will have a transmission coefficient proportional to the strength of the recording signal, (77). If this processed film is illuminated with a coherent optical phasefront, of sufficient extent to encompass the data collection length, the film will behave as an optical zone plate. The focal length of the zone plate will be proportional to R. Distance and wavelength scalings both come into play to scale the zone plate focal length from the radar range represented. The focal length of the zone

plate occurs at a position along the data track scaled from X_t. The zone plate has one dastardly fault in that both a real and virtual image are produced. A virtual image reconstructed wavefront appears to be diverging from a focal position behind the data film. A real-image reconstructed wavefront appears to be converging to a focus in the real space in front of the film. The two images are a manifestation of an ambiguity of the data (77), i.e., it could have been generated as we postulated, or in some other experiment where the sampled energy is converging to the target position. In the optical processor this ambiguity is handled by introducing a spatial carrier which forces the ambiguous images to propagate through the optical train along different paths with respect to the optical axis of the processor and allows the use of stops to block one of the images. The video of a chirp transmission will have the same form as (77) and indeed a dispersed chirped- range pulse can be recorded on film and processed optically because of the same zone plate properties. The zone-plate property of a recorded chirp signal explains the traditional use of chirp waveforms in SAR radars based upon optical processing. Other waveforms do not produce smooth optical wavefronts which can be compressed optically and the range data must be compressed before it is recorded on film. The aforementioned tilted plane [5] processor uses a combination of a one-to-one spherical telescope and a demagnifying cylindrical telescope to process appropriately scaled radar space data. The processing is the 2-D focusing of severely astigmatic signals.

The Fourier-transform (or inverse-transform) property of a lens can be explained in terms of its focal properties [10]. A lens will focus the energy in a planar wavefront, incident on its entrance pupil, to a diffraction-limited spot in the focal plane of the lens. The focus position is determined by the direction cosines of the incident wavefront. For a monotone such as (69) a linear film exposure produces a diffraction grating. An incident planar wavefront will be scattered into the ± 1 orders of this grating. Each order will be a planar wavefront which is focused to a spot by the lens. Again an offset is required to separate the ambiguous orders (images). In digital processing, the properties of quadrature signals are used to remove the ambiguous signal.

The nuances and limitations of optical processing are detailed subjects in their own right. This section has been included to provide an introduction to the concept of optical processing and not to debate its merit for radar processing. To date, film has been the sole media for recording the data from a wide-range swath. As 2-D spatial light modulators improve, optical processing of radar data in real time may become practical. However, even as our capability improves we will have to address topics such as: the practical dynamic range, the accuracy of this analog process, and the realization of practical apodizations to control sidelobe levels. We leave our discussions of the general properties of optical processing at this point. We will return to it as an element in a hybrid back-projection process which will be described later.

DISCRETE FOURIER TRANSFORMS

The ever increasing availability of digital processing power has lead to its near exclusive use in modern SAR implementations. The conceptual polar data space of the spotlight radar is no exception. In this section we will look at the mathematical nuances of processing the polar-formatted data form and the motivation for various implementation forms such as the discrete Fourier transform, and its efficient implementation in the FFT algorithm. The designation "Fourier transform" is used in a loose sense with preservation of the observable characteristics of a Fourier process and not necessarily the precise mathematics.

We recall that our interest is with the extraction of information from data with the residue form

$$S(x,y) = A_t \, e^{i[w_x X + w_y y]}$$

where x & y are cartesian coordinates mappable via a polar transformation to the radar frequency and a position in radar space. The Wx's and Wy's in a composite signal are to first order proportional to distances in radar space. To determine the strength of a return from a position represented by (Wx, Wy) we perform a matched filter operation on the residue signal, i.e.,

$$S(w_x, w_y) = S_i(x_t, y_t) = \iint S(x,y) e^{-i[w_x X + w_y y)} dx\,dy \qquad (79)$$

We recall that this matched filter form is ideally limited to a small neighborhood about some reference position. One can look at (79) and say that's a "Fourier transform." Mathematically it is not quite, as we see a minus sign in the kernal which is formally associated with the inversion or inverse Fourier transforms. Also, we ideally have infinite limits of integration and we are missing a scale factor of $1/2\pi$ [11]. However, all this is a "so what?" It is the form of (79) that is of interest. The result will have all the properties of an apodized Fourier transform, save for perhaps a scale factor and/or an axis inversion. The scale factor is not important as all targets are treated equally and relative values will remain. If the inversion of axis is a problem, we can work with the other

sideband of our analog IF chain and the phase $2k(r_o - r)$. It is not important if (80) is a Fourier Transform or not! We will illustrate below that all the techniques developed for Fourier processing are applicable to (79) and its basic properties are the same as those of a Fourier transform. Let's call it a

_____.

Going back to (79), and for purposes of illustration considering only one dimension, we have a signal form.

$$S_o(w) = \int S_i(x) e^{-iwx} dx \qquad (80)$$

We need only recall e^{-iwx} serves as a good approximation to the ideally matched filter for one of the many possible $S_i(x)$ making up our composite signal. The mathematical descriptions (79) and (80) indicate cumbersome processes in which the presence of each possible signal has to be probed with a new "kernal" e^{-iwx}. Let us seek an efficiency in a digital approximation to (80) by first noting that (80) is, in fact, a limiting definition of a summation process (Archimedes is credited with the conception)

$$S_o(w) = \text{limit}_{\Delta x_j \to o} \sum_j S_i(x) e^{iwx} \Big|_{x_j} \Delta x_j \qquad (81)$$

In this form we have put no restriction on the Δx_j's other than they all tend to zero before the summation, Σ, is equivalent to our integral, $\int$. Also, there is also no restriction on the extent of signal. Now let's say we don't go to the limit of (81) and are happy with

$$S_o(w) \approx \sum_j^N (Si(x) e^{-iwx})_{x_j} \Delta x_j \qquad (82)$$

where N reflects some finite number of samples over the field of the signal. A first implementation imposition generally comes in the form of a regular sampling, with the sampling rate tied to the frequency content of the signal. In the ideal limit of minimal sampling, we assume we have filtered and formatted our signals of absolute bandwidth B in frequency space into the zero centered band

$$-\frac{B}{2} \leq \nu_s \leq \frac{B}{2} \tag{83}$$

The maximum frequency content of any component of the signal is B/2. (The sorting of negative frequencies requires the quadrative channel.)
With this formatting we can sample at a rate

$$\nu_{sample} = \frac{1}{B} \tag{84}$$

and satisfy the minimal sampling requirement of at least two samples per wavelength of the highest frequency component in the signal. At this sampling rate (82) becomes

$$S_o(w) = \Delta_x \sum_{j=0}^{N-1} [S_i(w)e^{-iwx}]_{x=j\Delta x} \tag{85}$$

where

$$\Delta_x = \frac{1}{B} \tag{86}$$

and

$$N = \frac{L}{\Delta_x} = LB \tag{87}$$

The form of (85) has become a little more structured and we may also drop the scale factor. The minimal number of samples required is the space-bandwidth product of the signal, but this minimal number allowed only with the signals in the band of (83).

The above is beginning to introduce some structure into our estimation of $S_o(w)$, but it remains a tedious process. Let us now see what we may accomplish by introducing a structure into the w space. For one thing we know that W's of interest are limited by input bandwidth. We also know from our matched-filter process we

...e an uncertainty, and any input frequency may only be determined to an ...certainty.

$$\Delta\nu \geq \frac{1}{L} \tag{88}$$

because of our limited data aperture. Stated another way, for the form of (85) we cannot expect significant changes in the value of $S_o(w)$ on a scale less than the ... given above. This being the case, let us restrict our frequency space, w, interrogations to regular intervals, with (88) the upper bound on the length of these intervals. For our signal we can assume $w = 0$ is one position we wish to probe and may choose

$$w_k = k\Delta w = 2\pi \frac{k}{L} \tag{89}$$

with the result (85) may be manipulated into the form

$$S_o(k\Delta w) = \sum_{j=0}^{N-1} S_i(j\Delta x) e^{-i \frac{2\pi}{N} kj} \tag{90}$$

using various of the relationships expressed above. Inspection of (90) shows it has a periodicity of N with both k and j. These are manifestations of the process we are performing.

Let us consider the k periodicity. The signal $S_o(k\Delta w)$ is an estimate of the composite strength of frequency components in a subband in the original data set. This frequency component, which is real in our case, could also have been the result of an inadequate sampling of a higher signal frequency. The process does not know if the sampling is adequate or not, and for that matter, does not care, and will provide an output for all ambiguous signals which could produce the sampled data set. These ambiguous possibilities are the periodic repeats in w space. We know we have a bandlimited signal and as such only need consider N intervals of extent 1/L in a frequency band of extent B. The process sorts our data set of bandwidth

B into N bins of bandwidth $\Delta\omega$. With this sampling of data and frequency space, we see a need for a minimum of N samples in each space.

The periodicity in j can be explained by removing the summation in x, while retaining that in W. We now have a form

$$S_0(k\Delta w) = \int S_i(x) e^{-i\frac{2\pi xk}{L}} d_x \qquad (91)$$

In this form $S_0(k\Delta w)$ is the k^{th} coefficient of a complex Fourier series which we can use to represent the function $S_i(x)$ in the interval L [12], i.e.,

$$S_i(x) = \sum_{-\infty}^{\infty} S_0(k\Delta w) e^{i\frac{2\pi kx}{L}} \qquad (92)$$

Outside the interval L this $S_i(x)$ representation has a period of L or N ΔX. Thus, each interval L contains an identical signal, but again we don't care what the signal outside the interval may be as we will treat that in some other processing, if at all.

With this insight we see (90) provides us with estimates of the spectral content of a signal, $S_i(x)$, at discrete points within the frequency band of the signal. These estimates are in fact the coefficients for a finite Fourier series which may be used to represent the signal in this interval. We have a limited number of terms in this series, but have seen mathematical proof that, for a given number of terms, a finite Fourier series provides a minimum mean square estimate to $S_i(x)$. However, we can't locate a reference at this time.

Cleaning up (90) a little, we arrive at a discrete form

$$S_0(k\Delta w) = \sum_{j=0}^{N-1} S_i(j\Delta x) e^{-i\frac{2\pi}{N}jk} \qquad (93)$$

which provides an estimate of the composite signal strength in some subband Δw of the total signal bandwidth. Expression (93) is denoted as a discrete Fourier-transform. The form discussed above centered around N samples in frequency space. More samples may be considered with more processing. The minimal sample size N reflects the restraint physics (bandwidth and sample length) places on the rate of change of $S_o(w)$.

The complexity of (93) can be illustrated by writing the N possible forms of $(k \pm w)$ in a matrix form

$$\begin{bmatrix} S_o(1) \\ S_o(2) \\ \vdots \\ S_o(N) \end{bmatrix} = \begin{bmatrix} \\ a_{kj} \\ \\ \end{bmatrix} = \begin{bmatrix} S_i(1) \\ S_i(2) \\ \vdots \\ S_i(N) \end{bmatrix} \qquad (94)$$

where a_{kj} is an N x N matrix with elements of the form

$$a^{kj} = e^{-i\frac{2\pi}{N} kj} \qquad (95)$$

The array indicates the need for N complex operations for each of the N possible samples in frequency or on the order of N^2 complex computational operations to reduce the data set. The mathematics of Cooley and Tukey [13] and the efficiency of the FFT algorithm can be illustrated by considering the form of (94) when N is a power of 2. In this case, the regularity of $[a_{kj}]$ and its modulo 2π insensitivity permits the diagonalization of the matrix in $\log_2 N$ stages. The first stage of this process is the addition of row k to row k + N/2 and the subtraction of row k + N/2 from row k. The resulting form becomes

$$\begin{bmatrix} S'_o(1) \\ S'_o(2) \\ \vdots \\ S'_o(N) \end{bmatrix} = \begin{bmatrix} a'_{kj} & \vdots & 0 \\ \cdots & \vdots & \cdots \\ 0 & \vdots & a''_{kj} \end{bmatrix} \begin{bmatrix} S_i(1) \\ S_i(2) \\ \vdots \\ S'_i(N) \end{bmatrix} \qquad (96)$$

where $S_o'(j)'s$ are permutations of $S_o's$ and $S_i'(j)'s$ are now sums and differences of the original data signals. There are still N rows, but we now have two arrays of order (N/2) x (N/2). Another stage of operations on the $[a'kj]$ and $[a''kj]$ residue matrices will result in 4 arrays of order (N/4) x (N/4). The processes can continue to iterate through $\log_2 N$ such stages, until only diagonal elements remain in the N x N matrix relating N outputs to their unique N term weightings of the input data. The process exploits the fact that the N^2 processes indicated in (94), many times involve cases where a given data is operated on by the same weightings. The FFT tends to collect terms involving these common weightings early in the process and then fans out the result into latter stages of the process. An N point FFT can be implemented with an array of $(N/2 \log_2 N)$ Butterflies (Figure 10). A Butterfly accepts two complex input signals and uses one complex multiply and two complex adds to deliver two complex outputs to the next stage of the matrix diagonization process. The total process being completed using the order of

$$\frac{N}{2} \log_2 N \tag{97}$$

operations vs the N^2 indicated by (94).

The efficiencies of the FFT algorithm become even more pronounced when a two-dimensional filter is desired and we have to consider a 2-D discrete Fourier-transform form

$$S_o(k\Delta\omega, m\Delta\omega) = \sum_j^N \sum_l^N S_i(j\Delta x, k\Delta y) e^{i\frac{2\pi}{N}(kj + lm)} \tag{98}$$

Here a brute-force implementation indicates N^2 operations for each of the N^2 possible permutations of (k,m) where each has the range N. An FFT implementation is usually in the form of a series of operations. The first is an FFT of one data variable (j or l) for each of the other variables. This is the analog of sorting the data into range bins, and may indeed be a range-binning operation for a given radar processing operation. This still leaves N^2 input data points which are then processed with a second series of FFT's with the roles of j and l reversed (i.e., the azimuth processing of range-binned data). Each sequence requires

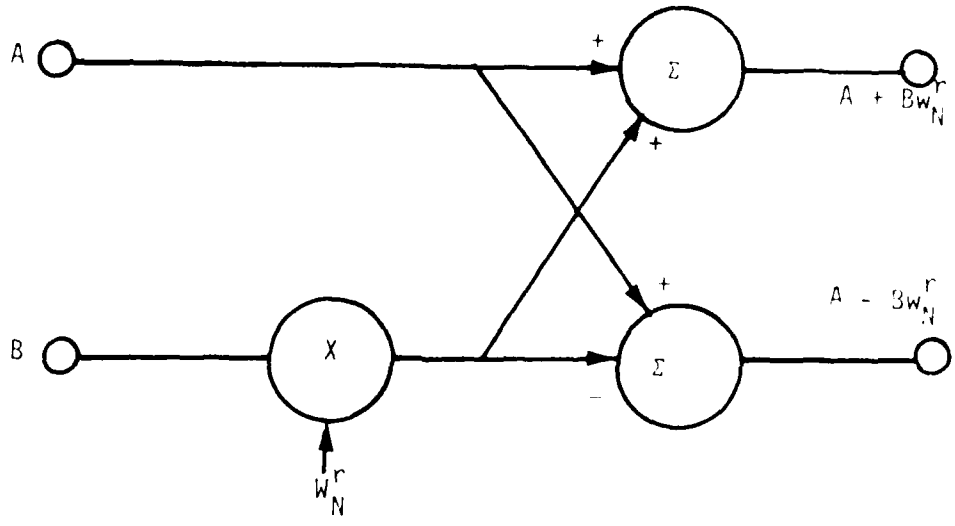

Figure 10. Complex Butterfly

$$\frac{N^2}{2} \log_2 N \qquad (\quad)$$

Butterfly operations, or a total of

$$N^2 \log_2 N \qquad (\quad)$$

for the complete filter. This compares to the N^4 operations indicated for a brute-force implementation. The motivation to use the FFT algorithm is obvious.

In this section we attempted to provide an introduction to digital SAR-matched-filter operations which take the form of a Fourier kernal, and give rise to an indicated need for "Fourier-transform" processing. In addition, we attempted to illustrate the order of complexity of a digital implementation of such a filter. We illustrated the mathematical basis of such filters and efficiencies which can accrue when regularities occur.

INTERPOLATION

In the preceding section we observed that the polar-formatted-SAR signals may be processed digitally, employing a discrete Fourier-transform algorithm. Relatively efficient FFT concepts may also be employed. However, the FFT implementations come with the burden of 2^b sample lengths and more importantly the need for regular samplings. For equal resolutions in range and azimuth, the data input to a 2-D FFT-based process has to be in the form of data values at points on a regular 2-D cartesian grid. The data collection produced values which in general may be randomly spaced, but are nominally along oblique straight and nonparallel lines. Centering the processing aperture on some segment of the data produces the requirement for estimates of the data values at points on a cartesian grid, given the data values along lines which appear to diverge from a common remote point. We assume that an oversample solution is not valid, i.e., we collect so much data that each cartesian point is assured of a data point in an acceptably near neighborhood. We could then select the data we desire and throw the remainder away. Rather than brute-force, let's just assume we have only an adequate sampling in a radial line format.

One method for the estimation of grid-point data is an interpolation based upon the data form. To good approximation the data form indicates an inverse Fourier-transform processing procedure. Thus, without stretching the imagination too far, we can say the data itself has the form of a Fourier transform of something which closely approximates the image we will produce. By placing a few restrictions on the data sets we can illustrate an interpolation process.

Consider the usual frequency-time Fourier-transform pair with a limited time sample transform

$$F(\omega) = \frac{1}{\sqrt{2\pi}} \int_{-T/2}^{T/2} e^{i\omega t} f(x)dx \qquad (1)$$

and its inverse

$$f(t) = \frac{1}{\sqrt{2\pi}} \int_{-\infty}^{\infty} e^{-i\omega t} F(\omega) d\omega \qquad (102)$$

We have produced estimates of F(w) at a series of points we may designate as w_j, but we really want estimates of points we may designate as β_k, i.e.,we simply go back and find

$$F(\beta_k) = \frac{1}{\sqrt{2\pi}} \int_{-T/2}^{T/2} f(t) e^{i\beta_k t} dt \qquad (103)$$

We may not be able to do this physically, but let's do it mathematically by noting our sample set wj should allow us to estimate the signal which created them or (drop 2π weighting)

$$f(t) \sim \sum_j F(\omega_j) e^{-i\omega_j t} \Delta w_j \qquad (104)$$

We have reconstructed the source of the original data and can use it in (103) to find

$$(F_{\beta_k}) = \int_{-T/2}^{T/2} e^{i\beta_k t} \left(\sum_j F(\omega_j) e^{-i\omega_j t} \Delta\omega j \right) dt$$

$$= \sum_j F(\omega_j) \Delta\omega_j \int_{-T/2}^{T/2} e^{it[\beta_k - \omega_j]} dt$$

$$= \Delta\omega_j T \sum_j F(\omega_j) \frac{\sin(\beta_k - \omega_j) T/2}{(\beta_k - \omega_j) T/2} \qquad (105)$$

In principle, the estimate of $F(\omega_k)$ is a weighted sum of all $F(w_j)$ samples and on the order of N operations are indicated for each desired data point. As a practical matter we see that only those samples within a frequency space resolution element contribute significantly to the estimate. For adequate sampling we would have two such points. It may be nice to add more by oversampling at the video and let the interpolation serve a presum, as well as a formatter function. Practical implementations obtain good estimates with only a near-neighborhood data set. For two-dimensional data, the indicated interpolation process is

$$f(\alpha,\beta) = \sum_m \sum_n F(\omega_m, \omega_n) \text{ sinc } (\alpha-\omega_m) \frac{T}{2} \text{ sinc } (\beta-\omega_m) \frac{T}{2} \qquad (106)$$

with N^2 operations of each of N^2 points in our minimally sampled case.

In one dimension we may alternately choose to implement an interpolation process based on a Taylor series representative of reasonably behaved data. We have data at position $f(x + nh)$ where n is an integer. We desire $f(x + \delta)$ where we can reasonably assume $\delta < h$. Using a Taylor series we find

$$f(x + \delta) = f(x) + f'|_x \delta + \frac{f''}{2!}|_x \delta^2 + \ldots \qquad (107)$$

and require estimates of f', f'', f''', etc, at x. Treating the available data in a Taylor or finite difference manner we have

$$f(x + nh) = f(x) + nh\, f'|_x + \frac{(nh)^2}{2!} f''|_x + \ldots \qquad (108)$$

It is possible to write a series of finite-difference equations using (108) and obtain estimates of the derivatives of f at x with even more accuracy as more of the neighborhood samples are involved. If a first- and second-order estimate is adequate, we find

$$f'|_x \approx \frac{f(x+h) - f(x-h)}{2h} \tag{109}$$

and

$$f''|_x \approx \frac{f(x+h) + f(x-h) - 2f(x)}{h^2} \tag{110}$$

We can proceed to estimates of higher order derivatives by considering more equations and sample points. The extension to two dimensions falls apart for the radar case as regular samples are generally not available in the orthogonal direction. We could associate a unique h with each data point, but the forms become more complex. The need for 2-D interpolations, i.e., consideration of diagonal elements vs sequential 1-D interpolations to estimate a data point value, is one of accuracy. The selection seems a matter of choice, and on the surface, appears to be a tradeoff between a near neighborhood and somewhat larger linear neighborhoods.

The above is an attempt to illustrate that a data set belonging to a well behaved process can be interpolated to another data set representing the same process. How this is done is not of particular import in this overview of the concepts of SAR. All we need to note is that our ideally formatted data indicated a minimal requirement for

$$N^2 \log_2 N \tag{111}$$

Butterflies to produce an $N \times N$ pixels image. We illustrated above that each of the required N^2 input data estimates will involve some number of operations. To definitively gauge the interpolation load, we would have to examine a given procedure in detail. For now, we need only note that the interpolation process dominates if its computational complexity for each of the N^2 data points exceeds the complexity of $\log_2 N$ Butterflies. The complexity may be some combinations of hardware and software. Interpolation has proven to be the dominating process in some recent SAR implementations and has prompted studies to reduce its intensity, or ideally to eliminate it by using alternative processing schemes which will not significantly increase the processing load too much beyond the equivalent of $N^2 \log_2 N$ Butterflies.

BACK-PROJECTION PROCESSING

This section is included to illustrate a variation which may be implemented to process the data. The appendix details another. They are offered as illustrations and not necessarily proposed as having merit. Back-projection processing is basically a piecewise evaluation of an integral or summation. For the cases of interest, we can consider the 1-D or 2-D discrete inverse Fourier transforms. In the 1-D case we can break the summation of (93) into a series of subintervals and estimate the desired quantity as

$$S_o(k\Delta\omega) = \sum_m S_o(k\Delta\omega)_m \qquad (113)$$

where $1 \leq m \leq N$. The quantities summed are the results of summing subintervals of the range of j or

$$S_o(k\Delta\omega)_m = \sum_{j_m}^{j_m+1-1} S_j(k\Delta\omega)e^{-i\frac{2\pi}{N}jk} \qquad (114)$$

where we designate the onset of a subinterval by j_m. It should be obvious that we can do this; however, the implementation is different. Implementing (93) using an FFT algorithm results in a rippling data-reduction sequence with the estimates $S_o(k\Delta\omega)$ appearing out of separate spigots some time later. The form of (113) illustrates that each subinterval provides a complex increment for our estimates of $S_o(k\Delta\omega)$, as did each term of (93). For each of the $k\Delta_w$ of interest a data store has to be established. The results of each subinterval summation is then added to the quantity already in store as a result of past subintervals summations. When all samples have been treated once, and only once, this sequential summation will produce the desired estimate (112). There are no restrictions on sample lengths.

The extension to two dimensions proceeds in the same manner; only now, the subintervals can be viewed as subareas of the total area of the data space. In this case we require a data store for each pixel in the final image array, $N_x \times N_y$ for what we have discussed above. The data aperture can be broken into as many nonoverlapping subareas as desired. The item of note is that the data store and its implied

to add a complex number to one already in store.

In the SAR arena, a one-dimensional optical spatial light modulator lends itself as a hybrid back-projector system, i.e., acousto-optic Bragg cell. It is conceptually feasible to reduce the polar-formatted-SAR data by sequential processings of the data in slightly wedged subareas of the data space as illustrated in Figure 11. In practice, those slices would be appropriately weighted samples of the data for any θ. For a chirp implementation, the data would be the baseband video of any radar PRF line superimposed on a carrier to separate the conjugate optical images produced by the Bragg cell when illuminated by a coherent wavefront. The complication for the optical processing is that a coherent detector array of N x N elements has to be provided. A spatially and temporarily coherent reference wavefront also has to be introduced before detection to extract both the amplitude and phase of the signal on each detector, for each subaperture. This is a major task. These amplitude and phase data are then supplied to the summing store associated with each detector.

The issues with back-projection processings should not be "are they are possible?" The issues are engineering attributes of any implementation. A major issue is the noise introduced by errors in the process; in particular, noise or extraneous signals which tend to be coherent and limit the potential $S/_N$ or dynamic ranges of the processed data. An example of such a coherent noise may be a ripple on a power supply common to many elements of a phased array, when components of each array element have a path delay which is voltage sensitive. The questions which have to be addressed in back-projection schemes center around how well a practical implement approaches the ideal of the iterative summation of (112) or its 2-D counterpart. These topics have their counterpart in digital processings where quantization levels and timings have to be addressed.

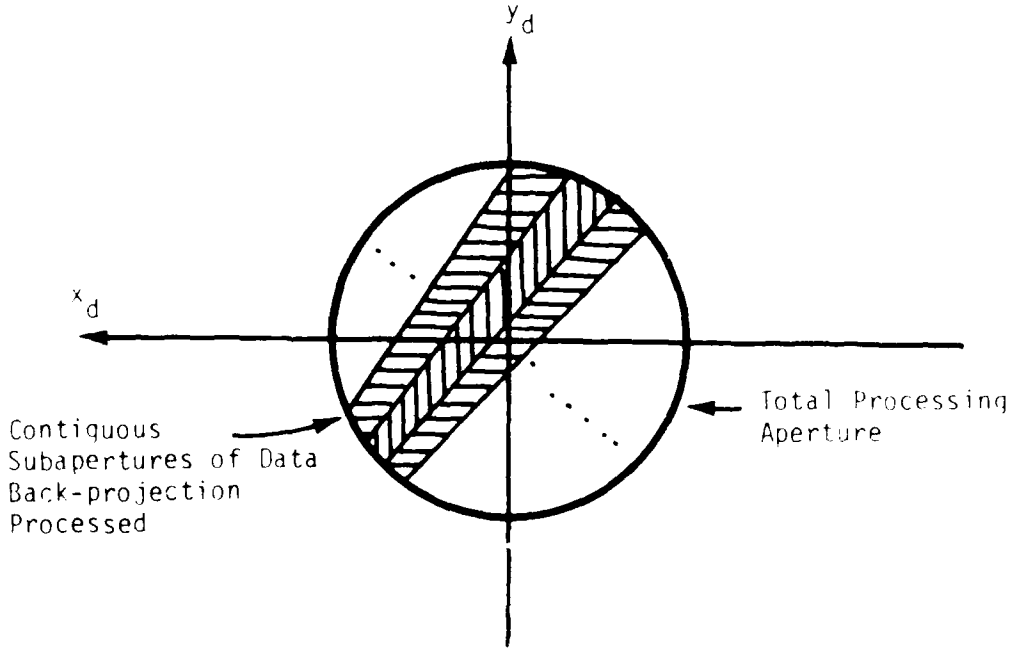

Figure 11. Back-Projection Subapertures in The Total Data Space Being Processed

DISCUSSION

The preceding discussion has separated the basic physical requirements of SAR from the engineering concerns which arise during any implementation of the process. We feel that the physics of such a radar are those of a microwave interferometer and a matched filter which can probe the data generated for the presence of a given signal. The implementation requirements of such an interferometer are easily specified and are built into any SAR. There are no basic restrictions on transmitted waveform or platform motion. The variations and activity in SAR centers more on the implementation of the matched filter, and it has at least been implied that these efforts are basic to a SAR. They are not.

Viewed with hind-sight, the development of SAR processing techniques seems to have evolved more along the lines of available techniques and the means to overcome the limitations of previous techniques. Initially all SAR data was optically processed and a range-azimuth data format was perhaps rather obvious. As digital processing was applied to strip-mapping SAR's the range-azimuth format remained. However, the azimuth data in any range bin was prefiltered so a batch process could be used to simultaneously extract the data on all azimuth cells in a given range bin. This afforded a computational efficiency since the same data did not have to be used in many processings as it is used in the optical processor, or as it would be used in a brute-force matched-filter implementation.

Range-azimuth formatting has remained the mainstay of SAR processing concepts, but imposes rather severe limitations on the data space which can be processed in a batch mode as resolutions improve. These limitations were first encountered during experiments with the rotary platform SAR emulator with its fine resolution capability. Attempts to overcome these limitations prompted the polar format observations of Walker. In the polar formatting procedure the matched filter for a reference position is removed from all data and the residue is conceptually mapped in a polar format for additional batch processing. During the collection of data for this format, individual scatter points may move through many resolution cells and a range-azimuth format becomes impossible. For points in the near neighborhood of the reference position, the frequency aspect-angle polar-formatted residue has the form of scatter-position-unique 2-D spatial monotones. The processing of these monotones is a 2-D spectral analysis of the data which exists in some aperture of the data

space. Much of the present activity in Spotlight SAR centers on the digital processing of this polar formatted data. The spectral analysis is rather nicely accomplished using implementations of the FFT algorithm. However, this algorithm comes with the burden of a particular sample length and regular data samples. The FFT's need for regular data samples forces an interpolation from measured values along polar lines to positions appropriate for the FFT algorithm processes. This interpolation tends to be more computationally intensive than the final data reductions with FFT's and has been the focus of considerable activity.

While the present focus on polar formatting, interpolation, and FFT algorithms is very well based, the purpose of this report is to illustrate that these are not fundamental radar processes. They are processes associated with a particular approximation to the ideal and as such come with their new set of limitations. These limitations are treated elsewhere. We feel that the report illustrates this position and also describes the basic characteristics involved in various implementation forms.

With the background and illustrations provided, a reader should be able to separate basic physical requirements from engineering considerations. The concepts of polar formatting are very powerful, and the use of FFT's to reduce the residual data may well be optimal in many situations where FFT's and their overhead are not optimal. The concepts, approaches, and procedures of this report may help to objectively access how best to approach the processing related aspects of a desired SAR implementation and not have to blindly accept approaches taken in past implementations, assuming them to be inviolate.

REFERENCES

[1] W.B. Davenport, Jr. & W.L. Rout, Random Signals and Noise, McGraw-Hill Book Company, New York, New York, 1958, Pg 246.

[2] ibid, pg 103.

[3] M. Born & E. Wolf, Principles of Optics, Pergamon Press, New York, New York, 1959, pg 418.

[4] W.M Brown & R.J. Fredricks, "Range-Doppler Imaging with Motion Through Resolution Cells," IEEE Trans. Aerosp. Electron. Syst., Vol AES-5, pp 98-102, Jan 1969.

[5] A. Kozma, E.N. Leith, & N.G. Massey, "Tilted-Plane Optical Processor," Applied Optics, Vol II, pp 1766-1777, 1972.

[6] W.J. Capriti, Jr., "Stretch: A Time-Transformation Technique," IEEE Trans. Aerosp. Electron. Syst., Vol AES-7, pp 269-278, March 1971.

[7] J.L. Walker, "Range-Doppler Imaging of Rotating Objects," IEEE Trans. Aerosp. Electron. Syst., Vol AES-16, pp 23-51, Jan 1980.

[8] J.L. Walker, Private Communication.

[9] L.J. Cutrona, E. Leith, C.J. Palermo, & L.J. Procello, "Optical Data Processing and Filtering System," IRE Trans. Information Theory, Vol IT-6, pp 386-400, June 1960.

[10] E.B. Champagne, "Transform Relations in Coherent Systems," Applied Optics, Vol 5, pg 1088, 1965.

[11] P.M. Morse & H. Feshback, Methods of Theoretical Physics, McGraw-Hill Book Company, New York, New York, 1953, pg 453.

[12] I.S. Sokolnikoff, Advanced Calculus, McGraw-Hill Book Company, New York, New York, 1939, pg 403.

[13] J.W. Cooley & J.W. Tukey, "An Algorithm for the Machine Calculation of Complex Fourier Series," Math. Comput., Vol 19, pp 296-301, 1965.

APPENDIX

Segmentation of the Discrete Fourier Transform

In this Appendix we will look at a segmentation approach to the discrete transform illustrated by (93). As in (93) an assumption of regular sampling is invoked. We will address the digital analogs of the multiple local oscillator radar, discussed in the section on Processing Considerations, which come about in an attempt to introduce batch processing to the range data.

Let us go by (93) and consider that for some reason we are interested in only M of the N possible estimates of $S_o(k\Delta w)$ given

$$S_o(k\Delta\omega) = \sum_{j=0}^{N-1} S_i(k\Delta x) e^{-i\frac{2\pi}{N}kj} \qquad (A-1)$$

The above represents an optimal sampling of the data space centered on zero frequency and an optimal sampling of frequency space to extract all significant data. Let us begin by assuming M is a power of 2 and the band of frequencies of interest are centered around $\nu = 0$. The process indicates M x N brute-force operations to accomplish the desired estimates.

How do we reduce this since we have an excess of data points for the band of frequencies of interest, but our sampling is driven by the input data? In our previous discussions, the analog sections of the radar provided IF filters and eliminated the uninteresting signals before we considered the frequencies of interest. Filtering can also be implemented digitally, and we can consider the result of summing b adjacent samples from a monotonic data set with a basic signal form

$$A_e^{iwt} \qquad (A-2)$$

where

$$-\frac{B}{2} \leq \frac{\omega}{2\pi} \leq \frac{B}{2} \text{ hertz} \qquad (A-4)$$

Sampling at a rate $\Delta_t = \frac{1}{B}$ and considering b samples beginning at time $t = t_0$ we arrive at a composite sum

$$S' = \sum_{0}^{b-1} e^{i\omega[t_0 tm\Delta t]} \qquad (A-5)$$

Performing the indicated summation yields

$$S' = e^{i\omega[t_0 + \frac{b-1}{2}\Delta t]} \frac{\sin\ (\frac{\omega b}{2})\ \Delta t}{\sin\ \frac{\omega}{2}\Delta t} \qquad (A-6)$$

Note that S' appears as a weighted sample of the original signal at time $t = t_0 + (\frac{b-1}{2})\Delta_t$. The weighting

$$\frac{\sin\ (\frac{\omega k}{2})\Delta t}{\sin\ (\frac{\omega}{2})\Delta t} \qquad (A-6)$$

is the array factor seen wherever multiple coherence signals interface, i.e., collections of microwave or optical sources which are arrayed in space and/or frequency. The weighting is frequency dependent with peak amplitudes of b at

$$\frac{\omega k t}{2} = n\pi,\ n = 0, \pm 1, \pm 2, \ldots \qquad (A-7)$$

For $\Delta T = 1/B$ we find peaks at mB. Our only interest is with the peak at $w = 0$ as our maximum frequency is $\pm B/2$. The 3-db width of the peak is approximately $\frac{5}{b}$, but the function (A-6) falls off relatively slowly and has significant sidelobes beyond B/b which may impact downstream processes.

To overcome the filter sharpness and sidelobe influence the samples can be weighted in amplitude before summation (Taylor, cosine squared, binomial, Tchebyscheff, etc.). The result of these weightings is a sharpening of the skirts of the array factor (analog of (A-6) for the particular weighting) and a virtual elimination of the sidelobes. These advantages come at the expense of a suppression of the peak amplitude ($w = 0$) by perhaps 1-2db and a slight broadening of the bandpass to something slightly greater than B/b. We have created a filter which preserves the strength of the signals in some band approximating B/b and have destructively interfered those outside this band.

For our case, (A1), we may want to do somewhat more than N/M of these presums along the data record length to provide data for our estimation of $S_o(k,w)$. This would be oversampling so that our estimates of the samples of interest would not have members too close to the skirts of the filter. To accomplish this, the blocks of data which are presumed, are separated by less than $b\,\Delta_t$, i.e., leading and trailing samples are components of two presums. The resultant M + samples may now be processed using an M + point FFT which requires on the order of

$$M \log_2 M \qquad \text{(A-8)}$$

operations. This may appear significantly less than the MN brute-force operations indicated. However, we have to include the presuming operations to see if we have gained anything. If we consider weighting and/or frequency shift to baseband (in general our subband may be anywhere in the total bandwidth) we will require on the order of Mb preconditioning or filtering operations for a total process approximating

$$M [\log_2 M + b] \qquad \text{(A-9)}$$

operations. As $N = Mb$ we may write (A-9) in the approximate form

$$N \left[\frac{\log_2 N - \log_2 b}{b} + 1 \right] \qquad \text{(A-10)}$$

The above indicates a potential for significant savings over a brute-force estimation of the M values of $S_o(k,w)$ which are of interest. However, if our interest is really with the full N values and the filtering was only an attempt to emulate the

analog functions of the radar, we lose. We would require b such procedures for the N total points of k Δ w. From A-10 we see the totality of operations would exceed the $N \log_2 N$ FFT operations indicated for the original data set.

This appendix has been included to provide a brief introduction to digital filtering and to further illustrate the power of efficient data reduction algorithms. On the surface it appears we would like to condition the input data for the largest possible FFT, or the total span of interest if we can build an arbitrary-sized FFT. If only a small portion of the collected data is of interest, filtering can provide efficiencies. A tradeoff may be possible if considerable conditioning has to be done on the raw signal, and the filtering operations can be incorporated into this process while incurring little addition complexity. We could be left with an N point FFT with its $N \log_2 N$ Butterflies, or b, M point FFT's with $N \log_2 M$ Butterflies where N = Mb. This is an analog of the radar case where we ignored the increased complexity of the analog sections of the radar and found our processing was minimized using the shortest possible FFT.

END

DATE

FILMED

DTIC

4/88